Vergleich der Abstandsmessung zwischen Zahnimplantat und gefährdeten Strukturen (Unterkiefernerv, Nasenboden und Nachbarzahn) in der Panoramaschichtaufnahme und der Digitalen Volumentomographie

Dissertation zur Erlangung des akademischen Grades
Doktor der Medizin (Dr. med.)

vorgelegt
der Medizinischen Fakultät
der Martin-Luther-Universität Halle-Wittenberg

von Annika Cecil Bertram
geboren am 22.11.1991 in Innsbruck, Österreich

Betreuer: Prof. Dr. med. Dr. med. dent. Alexander Walter Eckert

Gutachter:

- Prof. Dr. med. Alexey Surov, Magdeburg
- Prof. Dr. med. habil. Dr. med. dent. Matthias Schneider, Dresden

(14.09.2021)
(31.08.2022)

Referat

Die vorliegende kumulative Dissertation untersucht die Indikationen einer dreidimensionalen Bildgebung mithilfe eines Digitalen Volumentomogramms (DVT) zur Lagekontrolle eines dentalen Implantates in Relation zu den in der Implantologie gefährdeten Nachbarstrukturen N. alveolaris inferior, Nasenboden sowie Wurzel des Nachbarzahnes.

Hierzu wurden die Krankenakten einer Mund-Kiefer-Gesichtschirurgischen Praxis durchsucht, ob studienunabhängig Implantate in der Nähe von gefährdeten Strukturen sowohl in einem DVT als auch in der derzeitigen Standardaufnahme, einem konventionellen Orthopantomogramm (OPG), abgebildet worden waren. Die Abstände zu gefährdeten Strukturen wurden in beiden bildgebenden Verfahren gemessen, mit dem Bland-Altmann-Diagramm dargestellt und mit Hilfe der für die Einzelfragen bewährten statistischen Verfahren miteinander verglichen.

In der Nähe jeder der drei gefährdeten Nachbarstrukturen fielen besondere anatomische Regionen auf, in denen das DVT deutlich größere Abstände als das OPG zeigte: Im Bezug zum Mandibularkanal betrifft dies die Unterkiefer-Molarenregion in Relation zum Nasenboden die Oberkiefer-Eckzahnregion und im Bezug zur Nachbarzahnwurzel ebenso das Gebiet um den Oberkiefer-Eckzahn.

Besonders in diesen Regionen sollte bei Verdacht auf einen unzureichenden Abstand des Implantates zu gefährdeten Strukturen zusätzlich oder je nach intraoperativem Befund auch ersatzweise ein DVT veranlasst werden.

Bertram, Annika Cecil: Vergleich der Abstandsmessung zwischen Zahnimplantat und gefährdeten Strukturen (Unterkiefernerv, Nasenboden und Nachbarzahn) in der Panoramaschichtaufnahme und der Digitalen Volumentomographie, Halle (Saale), Univ., Med. Fak., Diss.,13 Seiten, 2021

Danksagung

Ein wissenschaftliches Projekt ist nie das alleinige Werk einer einzelnen Person, weshalb ich mich an dieser Stelle bei allen Menschen bedanken möchte, die mich auf meinem Weg zur Dissertation unterstützt haben.
Herr Prof. Dr. Dr. A. Eckert ermutigte mich von Anfang an und war mir eine stetige Hilfestellung in wissenschaftlichen und thematischen Fragen. Er hatte stets ein offenes Ohr für ungewöhnliche Ideen wie meine frühe Poster-Teilnahme auf dem „22nd International Congress of DentoMaxilloFacial Radiology“ in Philadelphia, USA. Nicht zuletzt der dortige Kontakt und Austausch mit Forschungsgruppen aus der ganzen Welt entfachte das Interesse an der Wissenschaft. Ich kann mir keinen motivierenderen Betreuer vorstellen und hoffe auf weitere spannende Gemeinschaftsprojekte in der Zukunft.
Herrn Univ.-Doz. Dr. Dr. R. Emshoff danke ich ebenso für seine geduldige und unerschöpfliche Unterstützung bei meinen ersten wissenschaftlichen Gehversuchen.

Außerdem möchte ich meinen 5 Geschwistern danken, welche mich immer wieder dazu ermutigen neue Wege einzuschlagen und gerade zu Beginn auch einmal gegen den Strom zu schwimmen. Mit meinen Eltern als weltbeste Fanbase meines Tuns und Seins möchte ich meine Danksagung beenden. Ohne ihre Liebe und Zuspruch (sowie zahlreiche Rechtschreibkorrekturen) wäre mein Promotionsprojekt nicht jenes geworden, das es heute ist. Danke.

Um Wiederholungen zu vermeiden, wird im Folgenden auf die Nennung der speziellen Aspekte der einzelnen Arbeiten mit ihren Literaturangaben verzichtet und vielmehr die Gemeinsamkeiten der Arbeiten herausgestellt.

Inhaltsverzeichnis

1. Einleitung und Zielstellung

Nach Einschätzung des ehemaligen Präsidenten der Deutschen Gesellschaft für Implantologie Prof. Schwarz wurden im Jahr 2018 deutschlandweit 1,3 Millionen dentale Implantate gesetzt [1]. In 0,5% der Fälle traten schwere intraoperative Komplikationen auf [2]. Zufallsbefunde einer Penetration des Implantats in die angrenzende anatomische Struktur sind mit 2,7 % nach D Clark et al. aber deutlich höher [3]. Ebenso zunächst symptomlose Penetrationen sollten zügig erkannt werden, da sich hieraus auch zeitverzögert Komplikationen entwickeln können.

Bei der Digitalen Volumentomographie (DVT) handelt es sich um ein dreidimensionales Schnittbildverfahren, mit dem Abstandsmessungen in allen Richtungen des Raumes möglich sind. Die Standardaufnahme zur Planung und Kontrolle der korrekten Lage von dentalen Implantaten ist immer noch das Orthopantomogramm (OPG), auch Panoramaschichtaufnahme. Es handelt sich um eine zweidimensionale Röntgenaufnahme des Ober- und Unterkiefers. Nachteil dieses Verfahrens scheint vor allem ihre Zweidimensionalität zu sein, die die Abgrenzung bei Überlagerungen und perspektivischen Fehlern nicht ermöglicht. Andere Nachteile wie unterschiedliche Vergrößerungsfaktoren können durch zusätzliche Maßnahmen wie die Anfertigung von Messaufnahmen minimiert werden.

Die Standardaufnahme (OPG) weist eine erheblich geringere Strahlenbelastung als die Digitalen Volumentomographie (DVT) auf. Bei der DVT ist diese je nach Gerät und Größe des Sichtfeldes (field of view, FOV) sehr unterschiedlich, bei vielen Standardeinstellungen etwa 5-mal so groß wie beim OPG.

Weiterhin sind DVT-Aufnahmen nach den Empfehlungen der Ärztekammer 7-fach teurer abzurechnen als die Standardaufnahme (OPG) [4]. Das führt zu häufigen Verweigerungen der Versicherungen, die Kosten für das DVT zu erstatten.

Daher sind Studien notwendig, die die Rechtfertigung einer Indikation zu der aufwendigeren Volumentomographie untersuchen.

Während man in Pubmed mehr als 800 Artikel über den Nutzen des DVTs vor einer dentalen Implantation findet, gibt es kaum Studien, die den Nutzen des DVTs als postoperative Röntgenkontrolle untersuchen.

Dabei ist sowohl für den Patienten als auch für den Operateur sehr wichtig, ob ein Implantat zu nah einer gefährdeten Struktur liegt oder ob es sich „nur“ um eine Überlagerung in einem zweidimensionalen Bild handelt.

Insbesondere sind folgende Strukturen gefährdet:

1. Der Nervus alveolaris inferior in seinem Canalis mandibulae.
2. Benachbarte Zahnwurzeln.
3. Der Nasenboden.
4. Der Mundboden nach Perforation der lingualen Knochenkompakta der Mandibula.
5. Die Schneider'sche Membran des Sinus maxillaris.

Zu 1: Die Schädigung des Nervus alveolaris inferior während der Implantatbett-Präparation oder des Setzens des Implantates kann unter Umständen eine nicht reversible komplette Taubheit der ipsilateralen Unterlippe einschließlich der Kinnhälfte zur Folge haben und ist deshalb als besonders schwerwiegende Komplikation einzustufen.

Zu 2: Die Schädigung des Nachbarzahns ist eine seltene, aber schwere Komplikation in der dentalen Implantologie. Je nach Schwere der Nachbarzahnschädigung kann eine Wurzelbehandlung oder sogar eine Entfernung des entsprechenden Zahnes notwendig werden.

Zu 3: Eine Penetration des Implantates in die Nasenhöhle kann folgenlos bleiben. Es ist jedoch ebenso möglich, dass es wegen einer Infektion über das Nasenlumen langfristig zu einem Verlust des Implantates kommt. Dies kann dann zu einer aufwendigen Neuversorgung führen. Insbesondere der Nasenboden als Risikostruktur gewinnt in den letzten Jahren eine zunehmende Beachtung. Gerade in Hinblick auf die Versorgung mit Sofortimplantaten, da diese für einen ausreichenden Halt gerne bis dicht an den Nasenboden gesetzt werden.

Bisher wurden die ersten 3 dieser Strukturen abschließend untersucht. Das Datenmaterial für Punkt 4 und 5 reicht meines Erachtens noch nicht für die Aufstellung einer fundierten These aus. Die Sammlung des Datenmaterials wird noch einige Zeit in Anspruch nehmen, da wie beim Antrag an die Ethikkommission versichert lediglich studienunabhängig angefertigte Röntgenaufnahmen verwendet werden.

Ziel der eingereichten Studien war es, die Abstände der Implantate zu gefährdeten Strukturen im OPG und DVT zu vergleichen und den Klinikern Orientierungshilfen an die Hand zu geben, durch die sie leichter bestimmen können, in welchen Fällen der zusätzliche Einsatz der DVT-Technologie gerechtfertigt sein könnte.

2. Diskussion

Den drei hier vorgelegten Publikationen ist gemeinsam, dass Abstände zwischen bereits gesetzten Implantaten und gefährdeten Nachbarstrukturen gemessen wurden – einmal im OPG und im Vergleich dazu im DVT. Die folgenden Absätze erläutern die Publikationen in dem Gesamtkonzept. Es wird ebenso auf relevante Literatur eingegangen, welche nach Einreichung der Arbeiten veröffentlicht worden ist.

2.1. Abstandsmessungen zum Nervus alveolaris inferior

Eine häufige und schwerwiegende Komplikation in der dentalen Implantologie ist die Schädigung des Nervus alveolaris inferior. Die gemessenen Abstände zwischen Implantat und dem Kanal des Nervus alveolaris inferior im OPG und DVT korrelierten miteinander. Das heißt, dass das OPG grundsätzlich geeignet für eine Abstandsmessung erscheint. Dennoch ist die Schätzung des tatsächlichen Abstandes der beiden Molaren zum Nervenkanal im OPG oft ungenau, insbesondere wenn das Implantat mit seinem apicalen Anteil lingual vom Nervenkanal liegt. In der zweidimensionalen Aufnahme kann man dies nicht erkennen; hier steht das Implantat vielmehr auf oder sogar im Kanal.

Bisher fehlte eine dedizierte wissenschaftliche Untersuchung, die solche Messungen in einzelnen Zahnregionen miteinander vergleicht. Im Allgemeinen stellt jedoch Angelopoulous et al. fest, dass das DVT dem digitalen OPG nachweislich in seiner diagnostischen Leistung überlegen ist [5]. Auch vermuteten M Gava et al. nach Analyse der Akten des zentralen finnischen Patientenversicherungszentrums einen Zusammenhang zwischen der Einführung des DVT und geringeren Ansprüchen wegen Behandlungsfehlern im Zusammenhang mit Zahnimplantatbehandlungen seitdem [6]. Dagegen kamen Vazquez et al. in ihrer Untersuchung zu dem Schluss, dass das OPG für die präoperative Planung der Implantatbehandlung in der Zahnmedizin ausreichend zu sein scheint, wenn ein Sicherheitsabstand von mindestens 2 mm über dem Mandibularkanal eingehalten wird [7]. In diesem Sinne empfiehlt sich auch weiterhin kein strahlenintensiveres DVT, solange im OPG ein ausreichender Abstand des Implantates gemessen wird. Bei kritisch geringen Abständen in der Standardaufnahme sollte jedoch ein DVT angefertigt werden, insbesondere in der Molarenregion.

2.2. Abstandsmessungen zum Nasenboden

In einer weiteren Publikation wurden die Abstandsmessungen des Implantates zum Nasenboden untersucht. Dieser Bereich gewinnt insbesondere durch den steigenden Anteil an Sofortimplantaten an Bedeutung, wobei die Implantate zum Erreichen einer ausreichenden Festigkeit weit bis an die Nasenhöhle herangesetzt werden müssen.

Alle gemessenen Abstände der 141 Implantate vom Nasenboden scheinen sich zunächst in beiden Röntgentechniken kaum zu unterscheiden, denn der Mittelwertsunterschied liegt bei 0,37 mm bei einer Standardabweichung von ± 1,73 mm.

Untersucht man jedoch die Abstände getrennt nach Zahnregionen, ergibt sich ein differenzierteres Bild:
Im Gegensatz zur Eckzahnregion zeigen die Messwerte in der mittleren und seitlichen Schneidezahnregion keinen bedeutsamen Unterschied.
Eckzahnregion: 41 Implantate, mittlere Differenz = -1,0mm, p =< 0,001
mittlere Schneidezahnregion: 49 Implantate, mittlere Differenz = 0,26 mm, p = 0,171
seitliche Schneidezahnregion: 50 Implantate, mittlere Differenz = -0,07mm, p = 0,727

Die Wahrscheinlichkeit, dass der im OPG gemessene Abstand mindestens 1 mm unter dem im DVT liegt, ist in der Eckzahnregion 5,4-fach so hoch wie bei den Schneidezähnen. Der größte negative Wert der Differenzen war im Eckzahnbereich zu verzeichnen (- 1,00 ± 0,72 mm). Das weist darauf hin, dass das OPG in diesem Bereich zu einer Unterschätzung des verfügbaren Knochens führt.

Wenn auch hier noch keine anderen Studien zum direkten Vergleich der einzelnen Regionen im OPG und DVT vorliegen, stellten schon andere Autoren wie Bouwens et al. die Problematik einer kieferorthopädischen Analyse der Wurzel der oberen Eckzähne im OPG dar [8]. Owens et al. weisen darauf hin, dass gerade in der Eckzahnregion unterschiedliche Gesichts- und Kieferformen und Einstellungsfehler zu Verzerrungen führen können, wenn der Eckzahn aus dem Schärfebereich des OPGs gerät. Auch wenn ein Implantat nach palatinal gekippt gesetzt wurde, kann sich die Implantatspitze vergrößert darstellen [9]. Weiterhin ist die anatomische Besonderheit dieser Region mit einem oft spitz zulaufenden kompakten Knochenareal zwischen Nase und Kieferhöhle zu beachten. Diese in unterschiedlichen Ebenen liegenden Objekte überlagern sich in der zweidimensionalen Darstellung. Siehe Peñarrocha M et al. [10].

Deshalb wird ein DVT immer dann empfohlen, wenn insbesondere in der oberen Eckzahnregion nach Anfertigung eines OPGs noch unklar ist, ob ein korrekter Abstand zum Nasenboden vorliegt. Es empfiehlt sich im Sinne eines abgestuften röntgendiagnostischen Konzeptes, siehe S. Haßfeld und U. Rother, zunächst ein OPG und erst bei unklaren Befunden ein DVT [11].

2.3. Benachbarte Zahnwurzeln

Eine weitere Studie untersuchte die Messdifferenzen zwischen Implantaten und benachbarten Zahnwurzeln im OPG und DVT.
Die deutlichste Unterschätzung des Abstandes im OPG zeigte sich zwischen Eckzahn und dem ersten Prämolaren mit einer mittleren Abweichung (MD) = - 1,11 mm und einer Standardabweichung (SD) von ± 1,08 mm bei N=161, gefolgt vom ersten zum zweiten Prämolaren mit einer Unterschätzung von MD = - 0,63 mm; SD = ± 1,24 mm bei N=76.

Tepedino et al. [12] beschrieben bereits eine generelle Unterschätzung des Abstandes der Wurzeln zueinander im OPG. Die hohe Differenz im Bereich des Eckzahns bis zum 1ten Prämolar ist nachvollziehbar, da der Zentralstrahl des OPG diese Region nicht rechtwinklig sondern distal exzentrisch durchläuft, auch wenn sich im Rahmen der technischen Weiterentwicklung und sich bewegender Rotantionszentren der Winkel einer senkrechten Ausrichtung immer mehr annähert. Pasler und Visser sprechen von einer dachziegelartigen Überlagerung der Prämolaren, wenn der Zentralstrahl distal exzentrisch eintrifft [13]. Dieser Effekt verstärkt sich, wenn Implantate in der Prämolarenregion zur Vermeidung einer Augmentation weiter nach palatinal gesetzt werden, während die Wurzel des Eckzahnes direkt hinter der bukkalen Knochenkompakta liegt.

Als Schlussfolgerung der gewonnenen Ergebnisse empfiehlt sich ein DVT zur Bestimmung des Abstandes zwischen Implantat und Nachbarzahn, bevor dieses bei einem zu geringen Abstand im OPG entfernt werden sollte, insbesondere in der Region vom Eckzahn bis zum 2ten Prämolaren.

2.4. Einschränkungen und wissenschaftliche Einordnung der Dissertation

Wie in den einzelnen Publikationen erwähnt müssen ebenso Einschränkungen der Studienergebnisse genannt werden. Alle Messungen wurden zwar zeitversetzt aber von „nur" einer Untersucherin an gleichen Röntgengeräten durchgeführt. Dadurch können systematische Fehler auftreten. Durch die Weiterentwicklung der Geräte können sich Änderungen ergeben, sowohl in der Genauigkeit der Darstellung als auch in der Strahlenbelastung. Daher sind die Ergebnisse nicht uneingeschränkt auf andere Geräte übertragbar [14].

Überdies ist nicht jede DVT-Aufnahme sicher auswertbar. Im Gegensatz zum OPG können hier Artefakte durch Absorption des Röntgenstrahls durch Materialien mit hoher Dichte wie Gold und Amalgam entstehen, oder ein Aufhärtungseffekt durch das „weiche" Titan kann die Ausmessungen erschweren [15].

Natürlich begleitet die Digitale Volumentomographie eine unerwünschte Strahlenbelastung, welche keineswegs sorglos und ohne spezifische Indikation angewandt werden sollte. Aus diesem Grund empfiehlt es sich bei der Entscheidung, ob eine zusätzliche DVT Aufnahme angefertigt wird, auch den intraoperativen Befund in Abhängigkeit von der Erfahrung des Implanteurs zu berücksichtigen [16]. Hinsichtlich der weiteren Entscheidung zur Behandlung, wie z.B. Entfernung des Implantates, vermag der bildmorphologische Befund die Einschätzung des erfahrenen Behandlers nicht zu ersetzen, sondern kann hier nur eine Entscheidungshilfe sein. Dennoch ist das DVT eine unabdingbare Stütze der heutigen dentalen Diagnostik.

Unter Leitung meines Betreuers Prof. Dr. med. Dr. med. dent. Alexander Eckert, damals kommissarischer Direktor der Mund- Kiefer- und Gesichtschirurgie der Martin-Luther-Universität Halle-Wittenberg, heute ärztlicher Direktor der Klinik für Mund-, Kiefer- und plastische Gesichtschirurgie der Universitätsklinik der Paracelsus Medizinischen Privatuniversität Nürnberg wurde das Promotionsprojekt geplant und realisiert.

Schlussendlich publizierte die Arbeitsgruppe mit mir als Erstautorin die Studien in drei Fachartikeln. Diese finden sich in englischsprachigen Journalen des Fachgebietes und haben ein Peer-Review-Verfahren durchlaufen. Die Zeitschriften kann man auch nach den Kriterien ihres Impaktfaktors (1,7, 1,9 und 2,4) als international angesehen einstufen. Selbstverständlich sind die Artikel in PubMed gelistet. Sie werden der Dissertationsschrift nachfolgend abgedruckt.

Nach drei weiteren promotionsunabhängigen in Pubmed gelisteten Publiktionen im Bereich der Schnittbilddiagnostik des Kiefergelenks konzentriert sich mein aktuelles Forschungsinteresse auf die strahlungsfreie dentale Bildgebung. Als Assistenzärztin der Neuroradiologie der Universitätsklinik Heidelberg unter Prof. Dr. med. Martin Bendszus laufen derzeit weitere Projekte zur magnetresonanztomografischen Darstellung von Zahn und Kiefer. Nicht zuletzt Erkenntnisse über Strahlenschäden mithilfe des Mikronukleustest (MNT) verstärken ein Interesse an strahlungsfreien Alternativen mitzuwirken. Santos MALd et al. nehmen in ihrer Meta-Analyse im Juli 2021 [17] an, dass es auch schon beim OPG zur genototoxischen Wirkung am oralen Epithel kommt, wenn auch derzeit die Evidenz gering ist.

3. Literaturverzeichnis

1. Presse-Information vom 30.11.2018 der Deutschen Gesellschaft für Implantologie zum 32. Kongress der DGI Schwarz, F [Konferenzbeitrag] 32. Kongress der Deutschen Gesellschaft für Implantologie Abgerufen 29. August 2021,https://www.dginet.de/documents/10164/1526375/PM_SCHWARZ.pdf/daa26dd8-0fe1-40b8-8969-f8e796623674

2. McDermott NE, Chuang SK, Woo VV, Dodson TB. Complications of dental implants: identification, frequency, and associated risk factors. Int J Oral Maxillofac Implants. 2003 Nov-Dec;18(6):848-55. PMID: 14696660.

3. Clark, D., Barbu, H., Lorean, A., Mijiritsky, E., & Levin, L. (2017). Incidental findings of implant complications on postimplantation CBCTs: A cross-sectional study. Clinical Implant Dentistry and Related Research, 19(5), 776–782.

4. Digitale Volumentomographie (DVT). (o. J.). Bundesaerztekammer.de. Abgerufen 29. August 2021, von https://www.bundesaerztekammer.de/aerzte/honorar/goae-ratgeber/abschnitt-o-strahlendiagnostik-nuklearmedizin-magnetresonanztomographie-und-strahlentherapie/digitale-volumentomographie-dvt/

5. Angelopoulous, C., Thomas, S. L., Hechler, S., Parissis, N., & Hlavacek, M. (2008). Comparison between digital panoramic radiography and cone-beam computed tomography for the identification of the mandibular canal as part of presurgical dental implant assessment. J Oral Maxillofac Surg, 66, 2130–5.

6. Marinescu Gava, M., Suomalainen, A., Vehmas, T., & Ventä, I. (2019). Did malpractice claims for failed dental implants decrease after introduction of CBCT in Finland? Clinical Oral Investigations, 23(1), 399–404.

7. Vazquez, L., Saulacic, N., Belser, U., & Bernard, J.-P. (2008). Efficacy of panoramic radiographs in the preoperative planning of posterior mandibular implants: a prospective clinical study of 1527 consecutively treated patients. Clinical Oral Implants Research, 19(1), 81–85.

8. Bouwens, D. G., Cevidanes, L., Ludlow, J. B., & Phillips, C. (2011). Comparison of mesiodistal root angulation with posttreatment panoramic radiographs and cone-beam computed tomography. American Journal of Orthodontics and Dentofacial Orthopedics: Official Publication of the American Association of Orthodontists, Its Constituent Societies, and the American Board of Orthodontics, 139(1), 126–132.

9. Owens, A. M., & Johal, A. (2008). Near-end of treatment panoramic radiograph in the assessment of mesiodistal root angulation. The Angle Orthodontist, 78(3), 475–481.

10. Peñarrocha, M., Carrillo, C., Boronat, A., & Peñarrocha, M. (2010). Maximum use of the anterior maxillary buttress in severe maxillary atrophy with tilted, palatally

positioned implants: a preliminary study. The International Journal of Oral & Maxillofacial Implants, 25(4), 813–820.

11. Haßfeld, S., & Rother, U. (2008). Röntgendiagnostik in der Mund-, Kiefer- und Gesichtschirurgie: Diagnose, Röntgenbefund, abgestuftes röntgendiagnostisches Untersuchungsspektrum, Schnittbilddiagnostik. Der MKG-Chirurg, 1(2), 137–147.

12. Tepedino, M., Cornelis, M. A., Chimenti, C., & Cattaneo, P. M. (2018). Correlation between tooth size-arch length discrepancy and interradicular distances measured on CBCT and panoramic radiograph: an evaluation for miniscrew insertion. Dental Press Journal of Orthodontics, 23(5), 39.e1-39.e13.

13. Pasler F, Visser H. (2003). Taschenatlas der Zahnärztlichen Radiologie, (1. Aufl.) Thieme (S. 38)

14. Lubbers, H.-T., & Dula, K. (Hrsg.). (2021). Digitale Volumentomographie (1. Aufl.). Springer.

15. Yepes, J. F., & Al-Sabbagh, M. (2015). Use of Cone-Beam Computed Tomography in Early Detection of Implant Failure. *Dental Clinics of North America*, *59*(ue 1), 41–56.

16. Bornstein, M. M., Scarfe, W. C., Vaughn, V. M., & Jacobs, R. (2014). Cone beam computed tomography in implant dentistry: a systematic review focusing on guidelines, indications, and radiation dose risks. Int J Oral Maxillofac Implants, 29 :55–77.

17. Santos MALD, Couto GR, Sabey MJS, Borges DPR, Takeshita. (2021). Can exposure to panoramic radiographs induce genotoxic effects on the oral epithelium? A systematic review with meta-analysis. Dentomaxillofac Radiol, 94, 20210149.

Die weiteren Literaturangaben sind aus dem Verzeichnis der einzelnen Publikationen zu entnehmen.

4. Thesen zur Dissertation

1. Die derzeitige Standardaufnahme zur Überprüfung der korrekten Lage eines Implantates ist das Orthopantomogramm (OPG), welches ein zweidimensionales Bild der Kiefer liefert. Die Digitale Volumentomographie bietet in einer Querschnittstechnik ein dreidimensionales Abbild des Sichtfeldes. Aufgrund der Möglichkeit von Überlagerungen im zweidimensionalen Bild ist das OPG daher anfälliger für Fehlbeurteilungen als das DVT.

2. Die Anfertigung eines DVTs bedeutet für den Patienten je nach Gerät und Einstellung ein Mehrfaches an Strahlenbelastung, weshalb der behandelnde Implantologe gemäß wissenschaftlich gestützten Indikationen entscheiden sollte, ob eine Bildgebung mittels DVT gerechtfertigt ist.

3. Klinisch relevant ist die Lagebeziehung eines Implantates zu gefährdeten Nachbarstrukturen wie dem Nervus alveolaris inferior, zu einer benachbarten Zahnwurzel sowie dem Nasenboden.

4. Nach den publizierten Ergebnissen dieses Promotionsprojektes bildet das OPG in speziellen Zahnregionen die Lagebeziehungen des Implantates zu möglicherweise gefährdeten Nachbarstrukturen nicht immer exakt genug ab, weshalb zusätzlich die Anfertigung eines DVTs indiziert ist, wenn im OPG kein adäquater Abstand zu den wichtigen Strukturen dargestellt werden kann.

5. Diess betrifft z.B. die Implantatsetzung in der maxillaren Eckzahnregion. Hier empfiehlt sich auf Grund der engen Lagebeziehung zu dem anatomisch variablen Nasenboden sowie Sinus maxillaris die zusätzliche Anfertigung eines DVTs, falls der Abstand im OPG zu gering erscheint.

6. In der Region des ersten und zweiten Molaren der Mandibula sollte nach Implantatsetzung bei kritischer Lagebeziehungen des Implantates zum Nervus alveolaris inferior im OPGs auch ein DVT angefertigt werden. Es zeigt sich dann häufiger ein ausreichender Abstand zum Nerven, denn nicht selten liegt die Implantatspitze lingual des Nervenkanales.

7. Implantate in der Prämolarregion, die im OPG eine zu enge Lagebeziehung zu der Eckzahnwurzel aufweisen, sollten zusätzlich mittels DVT dargestellt werden, da hier der schräg nach vorne gerichtete Strahlengang im OPG häufiger eine Überlagerung von Implantat und Wurzel vortäuscht.

Publikationsanteil

Bertram et al. Head & Face Medicine (2021) 17:19
https://doi.org/10.1186/s13005-021-00270-6

Head & Face Medicine

RESEARCH Open Access

Panoramic prediction equations to estimate implant- to-mandibular canal dimensions in the mandibular posterior region: implications for dental implant treatment

Annika Bertram[1], Alexander W. Eckert[2], Andreas Kolk[3] and Rüdiger Emshoff[3,4*]

Abstract

Background: To develop and cross-validate site-specific panoramic radiography (PAN) analysis prediction equations of implant-to-mandibular canal dimensions (IMCD) in mandibular regions posterior to the mental foramen, and to help determine in which instances CBCT technology will be a justified adjunct in clinical practice.

Methods: IMCD by PAN (Pan-D) from implant site-specific regions (first premolar, second premolar, first molar, and second molar sites) were collected from 40- to 70-year-old adolescents. They were randomly assigned to validation ($n = 144$) and cross-validation ($n = 148$) groups. The cone-beam computed tomography (CBCT) technique was used as the criterion method for the estimation of IMCD (CBCT-D). The PAN analysis equations were developed using stepwise multiple regression analysis and cross-validated using the Bland–Altman approach.

Results: There was a significant relationship between PAN-D and CBCT-D for both validation ($R^2 = 57.8$ %; $p < .001$) and cross-validation groups ($R^2 = 52.5$ %; $p < .001$). Root means-squared error (RMSE) and pure error (PE) were highest for the first molar (RMSE = 1.116 mm, PE = 1.01 mm) and the second molar region (RMSE = 1.162 mm, PE = 1.11 mm).

Conclusions: PAN-D has the potential to be developed as an indirect measure of IMCD. However, the findings suggest to exclude scoring of the first and second molars when assessing IMCD via PAN. Use of CBCT may be justified for all IMCD estimations in the first and second molars regions.

Trial registration: This study has been registered and approved by the Ethics Committee of the Martin-Luther University, Halle, Germany (2020-034).

Keywords: Dental implants, Mandibular edentulousness, Mandibular canal, Panoramic radiography, Cone-beam computed tomography

* Correspondence: ruediger.emshoff@tirol-kliniken.at
[3]University Clinic of Oral and Maxillofacial Surgery, Medical University of Innsbruck, Anichstraße 35, A-6020 Innsbruck, Austria
[4]Private Practice Oral and Maxillofacial Surgery, Freilassing, Germany
Full list of author information is available at the end of the article

Introduction

Dental implant surgery is associated with high success rates reported to range from 95.1 to 97 % [1, 2]. Nonetheless, in specific regions where the implant is inserted, anatomical structures may be injured, including adjacent teeth roots, lingual and/or buccal bone plates, maxillary sinus membranes, the nasal cavity floor, and the mandibular canal (MC) [3, 4].

With regard to the posterior mandible, preoperative cone-beam computed tomography (CBCT) assessment of the topographic relationship between the implant site and the MC, is an important aspect in treatment planning of standard implants in the posterior mandible [5, 6]. However, panoramic radiography (PAN) is considered to be the standard radiographic examination for implant treatment planning as it imparts a low radiation dose and gives the best radiographic survey [7–9]. According to previous studies, there is little consensus regarding how much information CBCTs can provide over conventional radiographs, and in which cases increased radiation exposure can be justified [10, 11]. To base clinical decisions regarding implant insertion in the posterior mandibular region from PAN findings, several studies tried to identify some predictive factors associated with alteration of the position of inferior alveolar nerve (IAN). Simonton et al. reported that both gender and age differences in the patient should be considered as a predictive factor in the relative location of the IAN compared with the roots of the mandibular first molar [12]. Moreover, the bucco-lingual IAN canal position was associated with ethnic factors and age according to the study by Levine et al. [13].

Even though many possible factors were evaluated as predictive ones, to our knowledge, there are no data available on the development and potential use of prediction equations for the estimation of implant-to-mandibular canal dimensions (IMCD) in dental implant patients. Therefore, the purpose of this study was to develop and cross-validate PAN analysis prediction equations of IMCD in mandibular regions posterior to the mental foramen, and to help determine in which instances CBCT technology will be a justified adjunct in clinical practice.

Materials and methods

Subjects

The subjects consisted of 81 consecutive adult patients (53 females; 28 males; average age 60.2 ± 11.3 years) referred to the practice of Oral and Maxillofacial Surgery, Freilassing, Germany for implant surgery. The subjects were informed about the study procedure and informed consent was received. This retrospective study followed the Declaration of Helsinki on medical protocol and ethics, and was approved by the Medical Ethical Committee of the Martin-Luther University Institutional Review Board (ethics approval No. 2020-034). Criteria for including a patient were (1) partially or totally edentulous in the mandibular premolar and/or molar regions, (2) age 18 years or older, and (3) additional need for dental implants or presence of post-implant complications requiring concurrent panoramic and CBCT imaging performed after the postsurgical phase of implant surgery. Criteria for excluding a patient were (1) unclear or distorted images (e.g., scattering, artifacts), (2) presence of metallic artifacts possibly impairing an accurate analysis, and (3) presence of pathologic changes in the region of interest. All patients were partially or totally edentulous in the mandibular premolar and/or molar regions. The patients received 292 Straumann® implants (Straumann AG, Basel, Switzerland), positioned in the posterior segment of the mandible. One hundred thirty-seven (47.0 %) implants were inserted in the premolar and 155 (53.0 %) in the molar region. All patients underwent PAN and CBCT. The CBCT technique was used as the criterion method for the estimation of IMCD.

Imaging

Digital PAN was taken using the Orthophos SL 3D (ORT, Sirona Dental Systems GmbH, Germany), operating at 60–90 kVp and 3–16 mA. For CBCT imaging, the same Orthophos SL 3D machine was used. The scanning settings were as follows: 5 × 5.5 cm field of view, 85 kV tube voltage, 6–7 mA tube current, a radiation time of 14.1, and a 0.12 mm pixel size. The radiographs were viewed with Galileos Implants and Sidexis 4.0 software (Dentsply Sirona). Subjects received only one dose of radiation for the CBCT, and the panoramic radiograph was generated from the CBCT scan.

Measurement Procedure

Implant sites (first premolar, second premolar, first molar, and second molar sites) were assessed on each panoramic- and CBCT radiograph. All radiographs were analyzed in standard conditions on a high-resolution gray-scale SMM Series monitor (Siemens AG, Karlsruhe, Germany).

The distance from the inferior border of the implant to the superior border of the MC was measured on panoramic radiographs, at sites corresponding to the first and second premolar implant site, and the first and second molar implant site. The multiplication factor was calculated for each implant by dividing the implant's measured length (in mm) on the postoperative panoramic radiograph by the implant's real length. The CBCT distances were measured on the correspondent bucco-lingual slices (Fig. 1). The measurements were made by a single examiner (AB), using a digital ruler graded in mm.

For assessment of intra-observer reliability, IMCD in the panoramic and CBCT images of 20 randomly selected

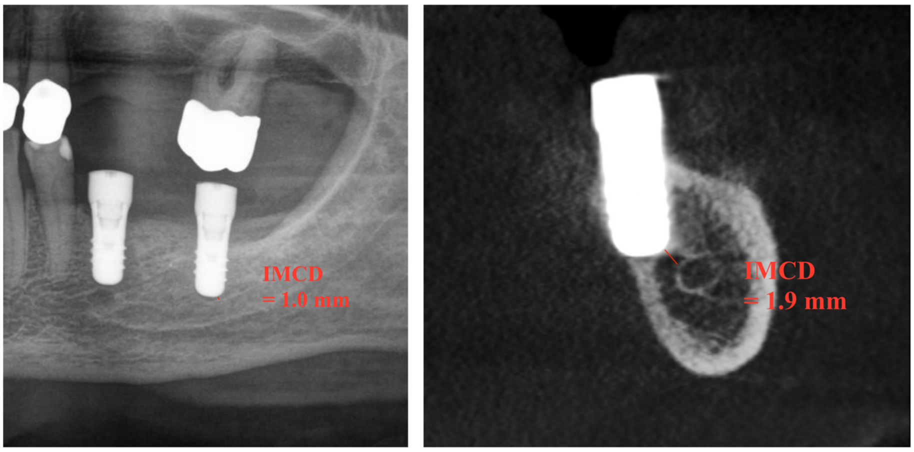

Fig. 1 Measuring technique of IMCD on PAN (**a**) and CBCT (**b**). Panoramic-like reconstructions visualize the MC in anterior-posterior direction (**a**). CBCT depicts the MC in buccolingual direction (**b**). After marking 1 point (voxel) each on the apex of the implant and the upper boarder of the MC, the computer calculated the shortest distance between these points to the nearest 0.1 mm. Optimal visualization was ensured by adjusting contrast and brightness of images with the image-processing software tool

cases were evaluated and measured by the investigator on two different days. For the panoramic and CBCT measurements, the mean differences were 0.069 ± 0.26 mm and 0.029 ± 0.35 mm respectively; the intra-class correlation coefficient for intra-observer agreement accounted for 0.975 and 0.984 respectively.

Statistics

Parameters were compared between validation and cross-validation groups using chi-squared test and paired t-test. In the validation group, stepwise multiple regression analysis was employed to develop PAN analysis equations. In a stepwise regression, those independent (predictor) variables are entered into the regression equation that contribute the most to the prediction of the dependent (predicted) variable. The resulting prediction equation predicts a value of the dependent variable for given values of the independent variables. IMCD derived from the CBCT method (CBCT-D) was used as dependent variable for the development of prediction equations separately. The independent variables included IMCD by PAN (Pan-D), age (to the nearest 1 year) and gender (male = 1, female = 0).

Multiple regression equations developed from the validation group were cross-validated on the cross-validation group. In cross-validation, a second set of data is used to assess the accuracy of an equation, i.e., quantitative criteria are provided to evaluate the equation's accuracy to predict outcomes in a new independent sample. Commonly used methods to assess predictive validity for continuous outcomes are the coefficient of determination (R^2), and the root mean squared error (RMSE). The R^2 describes the proportion of the variance in the dependent variable that is explained by the predictive model, i.e., values of R^2 closer to 1 indicate better prediction. The RMSE represents the square root of the differences between predicted and observed values, i.e., smaller values for RMSE indicate that the predicted values are closer to the observed ones and hence a better prediction.

IMCD assessed by the criterion method as well as the new prediction equations of the cross-validation group were compared using one-way analysis of variance (ANOVA). The pure error (PE) calculated as the square root of the mean of squares of differences between measured and predicted values was used to assess the performance of the prediction equations on cross-validation. The smaller the PE, the greater the accuracy of the equation [14].

Moreover, the approach of Bland and Altman was used to assess the agreement between PAN and CBCT methods. This statistical approach is recognized as the most appropriate way to compare the ability of different methods to measure the same parameter [15]. The Bland-Altman plot, or difference plot, was used to plot the differences between the PAN and CBCT methods against the averages of the two methods. Horizontal lines indicate the mean difference, and the 95 % limits of agreement, which are defined as the mean difference plus and minus 1.96 times the standard deviation of the differences [15].

Significance was set at $p < .05$. For the statistical analysis, the NCSS 2019 statistical software (NCSS, LLC. Kaysville, Utah, USA) was used.

Results

Subjects

There were 144 implants in the validation group, and 148 implants in the cross-validation group. There were no significant differences in variables of age, gender, and

Table 1 Characteristics of the study population

Variable	*Validation group (n = 144)*				*Cross-validation group (n = 148)*			
	1. P (n = 35)	*2. P (n = 33)*	*1. M (n = 45)*	*2. M (n = 31)*	*1. P (n = 35)*	*2. P (n = 34)*	*1. M (n = 43)*	*2. M (n = 36)*
Age (years) (mean ± SD)	58.7 (12.1)	61.8 (11.8)	57.7 (14.1)	61.2 (11.7)	60.0 (9.4)	60.9 (12.1)	57.7 (14.1)	63.8 (9.9)
Gender (n) (% female)	26 (74.3)	20 (60.6)	28 (62.2)	16 (51.6)	25 (71.0)	22 (62.9)	28 (65.1)	19 (52.8)
Implant-to-MC dimensions by PAN (mm) (mean ± SD)	2.7 (1.6)	2.7 (1.6)	2.5 (1.2)	2.3 (1.3)	2.7 (1.7)	2.7 (1.3)	2.5 (1.2)	2.4 (1.4)

MC mandibular canal; *PAN* panoramic radiography; *P* premolar; *M* molar; *n* number; *SD* standard deviation

PAN-D between tooth region-specific validation and cross-validation groups (Table 1).

Development of PAN analysis equations

A single equation was developed for the whole validation and cross-validation sample. Age and gender were no significant predictors of IMCD ($p > .05$), with PAN-D entering the models and explaining the largest variance of the models. There was a significant relationship between PAN-D and CBCT-D for both validation ($R^2 = 57.8\,\%$; $p < .001$) and ($R^2 = 52.5\,\%$; $p < .001$) cross-validation groups. This shows that PAN-D has the potential to be developed as an indirect measure of IMCD. The PAN analysis prediction equation for the estimation of IMCD for the validation group was as follows: IMCD = 0.812 x PAN-D + 0.674 ($R^2 = 0.578$), and for the cross-validation group as follows: IMCD = 0.744 x PAN-D + 0.762 ($R^2 = 0.525$).

Implant site-specific sets of preliminary equations were constructed for the prediction of IMCD. In each set the equations were constructed using PAN-D as an independent variable. Implant site-specific PAN analysis prediction equations for CBCT-D were able to predict 41.0–77 % of variances, while RMSE showed the highest values for the first molar (1.116 mm) and second molar region (1.162 mm) (Table 2).

Cross-validation of the equations

The developed regression equations were applied to the cross-validation group to evaluate their accuracy. No significant difference between measured and predicted values for each tooth region was found ($p > .05$) (range of bias, -0.04 mm to 0.30 mm) (range of PE, 0.00 mm to 1.11 mm). The highest PE was found for the first molar (1.01 mm) and second molar region (1.11 mm) Measured values strongly correlated with predicted values (range of r, 0.693 to 0.885, $p < .001$) for IMCD (Table 3).

The linear relationship beween measured and predicted IMCD, and the difference between measured and predicted IMCD plotted against the mean of the predicted and measured IMCD are shown in Figs. 2, 3, 4 and 5. Bland-Altman analyses showed lowest agreement between predicted and actual IMCD for the first molar (limits of agreement, -2.35 mm to 1.89 mm) and second molar region (limits of agreement, -2.08 mm to 2.20 mm). A total of 4 implant-sites (2.7 %), whose differences exceeded the 95 % confidence limits of IMCD, were identified.

Table 2 Tooth-region specific equations for the prediction of IMCD derived from validation group

Tooth Region	*Equation*	R^2	*RMSE (mm)*
1. Premolar	CBCT-D = 0.877 + 0.712 PAN-D	0.614	0.858
2. Premolar	CBCT-D = 0.172 + 0.970 PAN-D	0.774	0.873
1. Molar	CBCT-D = 0.744 + 0.794 PAN-D	0.571	1.116
2. Molar	CBCT-D = 1.384 + 0.735 PAN-D	0.409	1.162

CBCT-D Implant-to-MC dimensions by cone-beam computed tomography; *PAN-D* Implant-to-mandibular canal dimensions by panoramic radiography; *P* premolar; *M* molar; *RMSE* root means-squared error; *n* number; *SD* standard deviation

Discussion

Considering the fact that lesions to the IAN are reported as the most frequent and severe complications associated with implant surgery [16–20], it makes it necessary to assess the topographic relationship between the implant site and the MC preoperatively. Damages to the alveolar nerve that do occur during implant surgery procedures may be limited by careful preoperative depiction of the MC on imaging examinations, since the available bone height of the edentulous site is determined by the distance between the alveolar ridge and the MC. Imaging techniques such as PAN [8, 21–23] conventional tomography [21], CT [22], and CBCT [9, 24–26] have been used to depict the course of the MC. Compared to 2-dimensional techniques, use of CBCT avoides the occurrence of superimposition of anatomic structures, and the effect of image magnification. In addition, advantages of CBCT over CT include short scanning time, up to 15 times lower effective lower radiation doses, and easier image acquisition [26]. With this imaging mode becoming increasingly more usable in dental and maxillofacial practices [9, 24–26], it has been argued that this technique could provide valuable information about the location of the MC in vertical and horizontal planes, thereby allowing to insert appropriate sized implants in otherwise underestimated [27, 28] or overestimated regions [29].

Table 3 Implant-to-mandibular canal dimensions assessed by criterion method and each of the PAN equations

Tooth Region	*Mean (mm)*	*95 % CI for the mean*	*Correlation[a](r)*	*Mean bias (mm)*	*Pure error (mm)*
1. Premolar (*n* = 35)					
Criterion method (CBCT)	2.9 ± 1.5	2.35–3.40			
PAN equation	2.9 ± 1.2	2.52–3.32	0.737	− 0.04 ± 1.03	0.00
2. Premolar (*n* = 34)					
Criterion method (CBCT)	3.1 ± 1.8	2.48–3.70			
PAN equation	2.8 ± 1.2	2.37–3.21	0.818	0.30 ± 1.04	0.29
1. Molar (*n* = 43)					
Criterion method (CBCT)	2.5 ± 2.1	1.90–3.16			
PAN equation	2.8 ± 1.7	2.26–3.29	0.885	− 0.26 ± 0.99	1.01
2. Molar (*n* = 36)					
Criterion method (CBCT)	3.2 ± 1.5	2.70–3.70			
PAN equation	3.1 ± 1.1	2.75–3.47	0.693	0.06 ± 1.09	1.11

CBCT cone-beam computed tomography; *PAN* panoramic radiography; *P* premolar; *M* molar; [a] correlation between criterion method and assessments made by each of the prediction equations

However, Angelopoulos et al. [17] stated that even though CBCT has been proven to be superior in diagnostic performance to digital PAN, CBCT should not necessarily replace digital PAN due to the fact that use of CBCT is associated with a 4–20 times higher radiation exposure. Further, Frei et al. [7] who performed a study on the necessity for cross-sectional imaging of the posterior mandible for treatment planning in implant dentistry concluded that preoperative cross-sectional spiral tomography imaging did minor impact on treatment planning and the selection of implant diameter and length. In their investigation Vazquez et al. [30] came to the conclusion that PAN appears to be sufficient for preoperative implant treatment planning in the mandibular posterior region, i.e. cross-sectional imaging techniques may not be necessary, if a safety margin of at least 2 mm above the MC is maintained.

The current study developed PAN analysis prediction equations for the estimation of IMCD in the posterior mandible to the mental foramen. To the best of our knowledge, this is the first study to develop a PAN equation for adults across tooth region-specific groups. The developed PAN equations showed comparatively minor predictive performance for the first molar (R^2 = 57 %, RMSE = 1.12 mm) and the second molar region (R^2 = 41 %; RMSE = 1.16 mm). Further, the validation results indicated that PE and bias were comparatively higher for these regions,

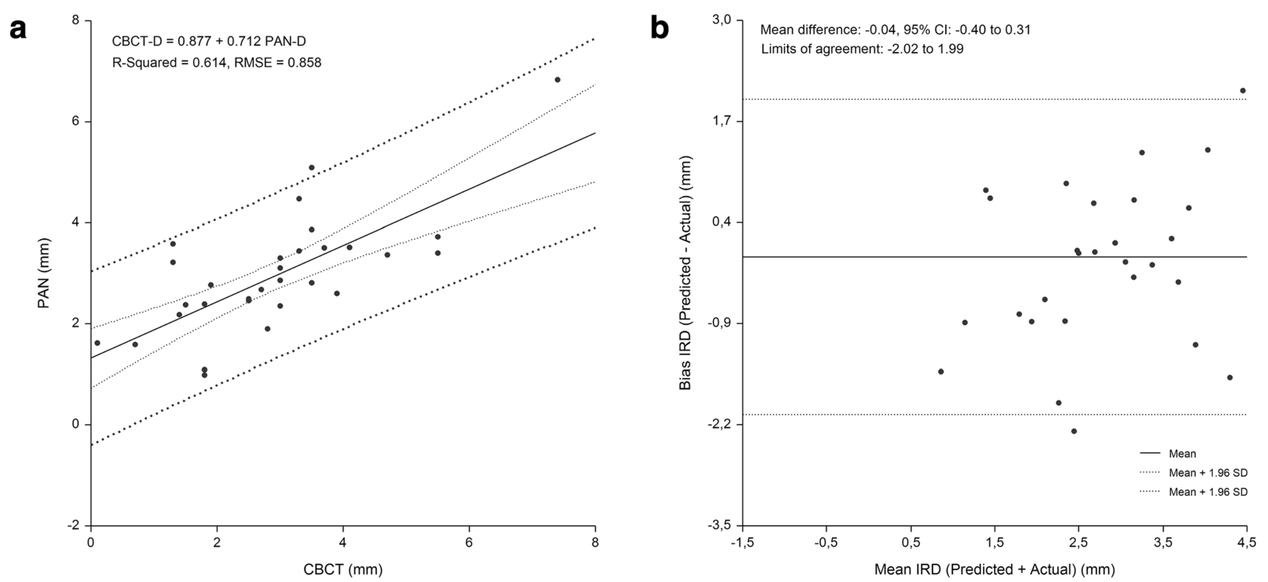

Fig. 2 First premolar region. Linear regression (**a**) and Bland Altman analysis (**b**) of the relationship beween IMCD assessed by PAN analysis prediction equation and criterion (CBCT) method. RMSE = 0.858 mm, mean bias = -0.04 mm and PE = 0.00 mm

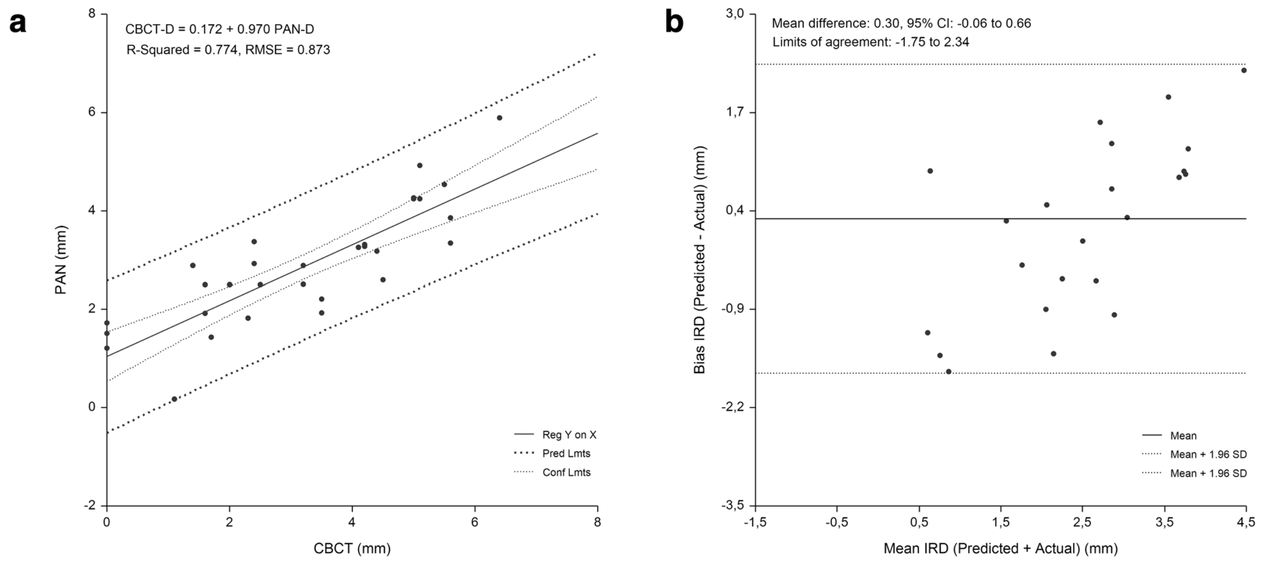

Fig. 3 Second premolar region. Linear regression (**a**) and Bland Altman analysis (**b**) of the relationship beween IMCD assessed by PAN analysis prediction equation and criterion (CBCT) method. RMSE = 0.973 mm, mean bias = 0.30 mm and PE = 0.29 mm

while the limits of agreement assessed by Bland–Altman approach showed comparatively wider ranges. These data support the contention to exclude scoring of the first and second molars when assessing IMCD via PAN [31]. Further, these findings may suggest that the respective equations may not be used in a community or clinical setting when CBCT techniques are not available. However, the accuracy of an equation usually change when it is applied to other samples. Hence, population-specific PAN prediction equations may have to be developed and validated considering the age-, gender-, ethnic- and anatomy-related factors contributing to MC variations [11, 13, 32].

In implant dentistry, CBCT imaging has been considered a highly accurate treatment planning tool for the performance of reliable linear measurements [8, 33] However, there are several factors such as machine characteristics, radiation exposure, and image-processing software that may affect the accuracy of reformatted CBCT images [34, 35]. In a recent systematic review of the available evidence on the accuracy of linear

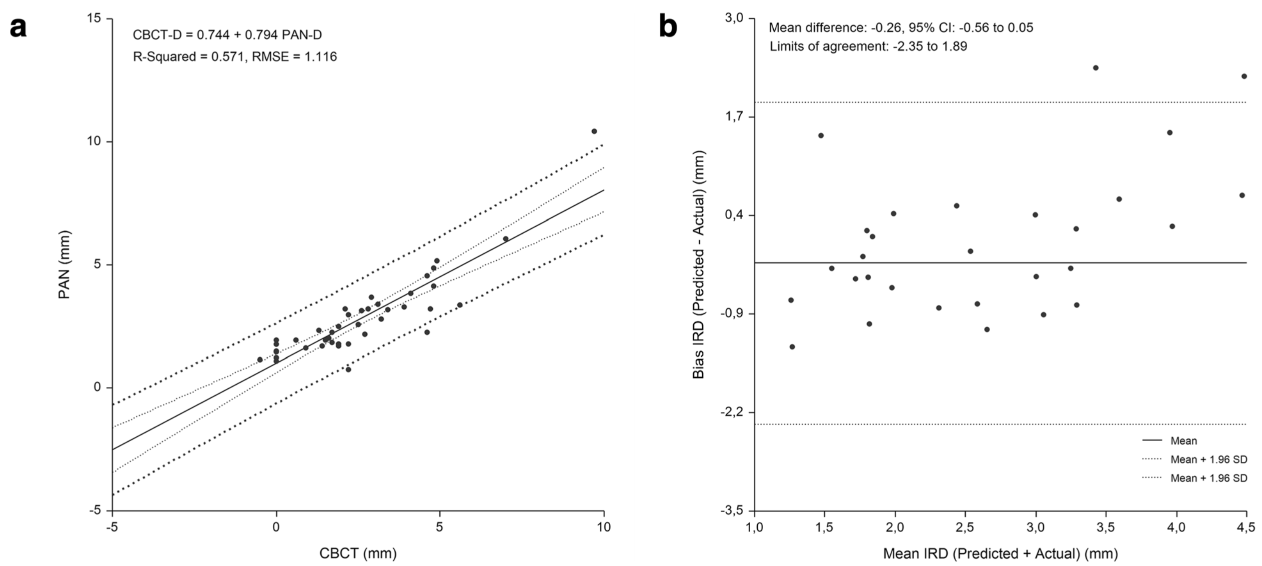

Fig. 4 First molar region. Linear regression (**a**) and Bland Altman analysis (**b**) of the relationship beween IMCD assessed by PAN analysis prediction equation and criterion (CBCT) method. RMSE = 1.116 mm, mean bias = -0.26 mm and PE = 1.01 mm

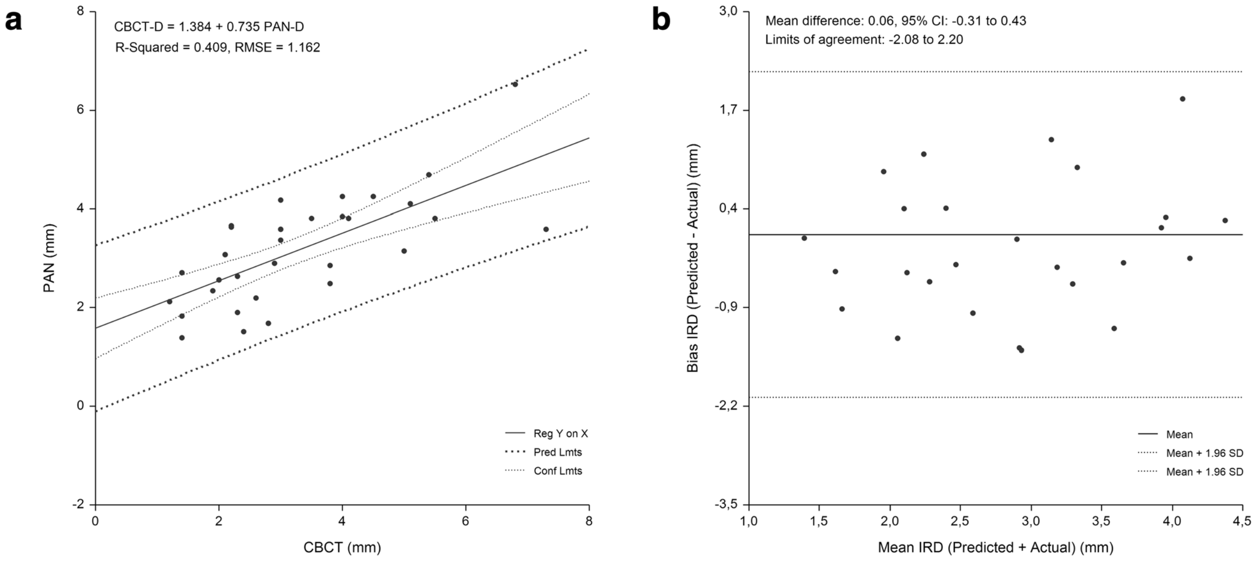

Fig. 5 Second molar region. Linear regression (**a**) and Bland Altman analysis (**b**) of the relationship beween IMCD assessed by PAN analysis prediction equation and criterion (CBCT) method. RMSE = 1.162 mm, mean bias = 0.06 mm and PE = 1.11 mm

measurements when using maxillofacial CBCT specifically in the field of implant dentistry [36], the authors reported that most studies showed submillimeter accuracy of CBCT measurements compared to a gold standard, while there was no clear trend as to whether measurements are consistently under- or overestimated.

The present study needs to be evaluated in the context of some limitations. First, measurements were made by a single observer, i.e. observer bias could have occurred in the data collection process. This error may be reduced by study designs incorporating two or more observers and a multi centre setting, and having their measurements compared and correlated statistically. Second, missing dentitions could have an underestimated effect on mandibular canal morphology, i.e. ridge resorption and bone remodeling following dental extraction may potentially affect the position of the mandibular canal. Third, use of CBCT imaging could have produced artifacts caused by high-density metal materials such as dental implants. Beam hardening and scattering effect artifacts could have reduced the contrast, thereby impairing the detection of structures of interest and as a result producing errors when performing linear measurements on CBCT images [37, 38].

Conclusions

PAN-D has the potential to be developed as an indirect measure of IMCD. However, the findings suggest to exclude scoring of the first and second molars when assessing IMCD via PAN. Use of CBCT may be justified for all IMCD estimations in the first and second molars regions.

Abbreviations

ANOVA: One-way analysis of variance; CBCT: Cone-beam computed tomography; CBCT-D: IMCD assessed by CBCT; IAN: Inferior alveolar nerve; IMCD: Implant-to-mandibular canal dimensions; MC: Mandibular canal; PAN: Panoramic radiography; PAN-D: IMCD assessed by PAN; RMSE: Root mean square error; PE: Pure error

Acknowledgements

Not applicable.

Authors' contributions

AB and AWE collected the data, contributed to drafting the article; RE developed the design, analyzed the data, contributed to drafting and critical revision of the article; AK contributed to critical revision of the article. The author(s) read and approved the final manuscript.

Funding

This research did not receive any specific grant from funding agencies in the public, commercial or not-for-profit sectors.

Availability of data and materials

Due to the nature of this research, participants of this study did not agree for their data to be shared publicly, so supporting data is not available.

Declarations

Ethics approval and consent to participate

The study is in accordance with the ethical standards of the Helsinki declaration and was approved by the ethics committee of the Martin-Luther University, Halle, Germany (2020-034).

Consent for publication

Not applicable.

Competing interests

The authors declare that they have no competing interests.

Author details

[1]Otto von Guericke University of Magdeburg, Magdeburg, Germany. [2]University Clinic of Oral and Maxillofacial Surgery, Martin-Luther University, Halle-Wittenberg, Germany. [3]University Clinic of Oral and Maxillofacial

Surgery, Medical University of Innsbruck, Anichstraße 35, A-6020 Innsbruck, Austria. [4]Private Practice Oral and Maxillofacial Surgery, Freilassing, Germany.

Received: 25 August 2020 Accepted: 11 May 2021
Published online: 09 June 2021

References

1. Goodacre CJ, Bernal G, Rungcharassaeng K, Kan JY. Clinical complications with implants and implant prostheses. J Prosthet Dent. 2003;90:121–32.
2. Quirynen M, De Soete M, van Steenberghe D. Infectious risks for oral implants: A review of the literature. Clin Oral Implants Res. 2002;13:1–19.
3. Clark D, Barbu H, Lorean A, Mijiritsky E, Levin L. Incidental findings of implant complications on postimplantation CBCTs: a cross-sectional study. Clin Implant Dent Relat Res. 2017:19: 776–82.
4. Misch K, Wang H-L. Implant surgery complications: etiology and treatment. Implant Dent. 2008;17:159–68.
5. Rios HF, Borgnakke WS, Benavides E. The Use of Cone-Beam Computed Tomography in Management of Patients Requiring Dental Implants: An American Academy of Periodontology Best Evidence Review. J Periodontol. 2017;88:946–59.
6. Tyndall DA, Brooks SL. Selection criteria for dental implant site imaging: a position paper of the American Academy of Oral and Maxillofacial Radiology. Oral Surg Oral Med Oral Pathol Oral Radiol Endod. 2000;89:630–7.
7. Frei C, Buser D, Dula K. Study on the necessity for cross-section imaging of the posterior mandible for treatment planning of standard cases in implant dentistry. Clin Oral Implants Res. 2004;15:490–7.
8. Harris D, Buser D, Dula K, et al. E.A.O. guidelines fo the use of diagnostic imaging in implant dentistry. A consensus workshop organized by the European Association for Osseointegration in Trinity College Dublin. Clin Oral Implants Res. 2002;13:566–70.
9. Dula K, Mini R, van der Stelt PF, Buser D. The radiographic assessment of implant patients: decision-making criteria. Int J Oral Maxillofac Implants. 2001;16:80–9.
10. Bornstein MM, Scarfe WC, Vaughn VM, Jacobs R. Cone Beam Computed Tomography in implant dentistry: a systematic review focusing on guidelines, indications, and radiation dose risks. Int J Oral Maxillofac Implants. 2014;29 Suppl:55–77.
11. De Vos W, Casselman J, Swennen GR. Cone-beam computerized tomography (CBCT) imaging of the oral and maxillofacial region: a systematic review of the literature. Int J Oral Maxillofac Surg. 2009;38:609–25.
12. Simonton JD, Azevedo B, Schindler WG, Hargreaves KM. Age- and gender-related differences in the position of the inferior alveolar nerve by using cone beam computed tomography. J Endod. 2009;35:944–49.
13. Levine MH, Goddard AL, Dodson TB. Inferior alveolar nerve canal position: a clinical and radiographic study. J Oral Maxillofac Surg. 2007;65:470–4.
14. Guo SS, Chumle WC. Statistical methods for the development and testing of predictive equations. In: Roche AF, Heymsfield SB, Lohman TG, editors. Human Body Composition. Champaign: Human Kinetics; 1996. pp. 191–202.
15. Bland JM, Altman DG. Statistical methods for assessing agreement between two methods of clinical measurement. Lancet. 198;61:307–10.
16. Alhassani AA, AlGhamdi AS. Inferior alveolar nerve injury in implant dentistry: diagnosis, causes, prevention, and management. J Oral Implantol. 2010;36:401–7.
17. Angelopoulous C, Thomas SL, Hechler S, Parissis N, Hlavacek M. Comparison between digital panoramic radiography and cone-beam computed tomography for the identification of the mandibular canal as part of presurgical dental implant assessment. J Oral Maxillofac Surg. 2008;66:2130–5.
18. Burstein J, Mastin C, Le B. Avoiding injury to the inferior alveolar nerve by routine use of intraoperative radiographs during implant placement. J Oral Implantol. 2008;34:34–8.
19. Ellies LG, Hawker PB. The prevalence of altered sensation associated with implant surgery. Int J Oral Maxillofac Implants. 1993;8:674–9.
20. Wismeijer D, van Waas MA, Vermeeren JI, Kalk W. Patients' perception of sensory disturbances of the mental nerve before and after implant surgery: a prospective study of 110 patients. Br J Oral Maxillofac Surg. 1997;35:254–9.
21. Lindh C, Petersson A. Radiologic examination for location of the mandibular canal. a comparison between panoramic radiography and conventional tomography. Int J Oral Maxillofac Implants. 1989;4:249–53.
22. Naitoh M, Katsumata A, Kubota Y, Hayashi M, et al. Relationship between cancellous bone density and mandibular canal depiction. Implant Dent. 2009;18:112–18.
23. Tantanapornkul W, Okouchi K, Fujiwara Y, et al. A comparative study of cone-beam computed tomography and conventional panoramic radiography in assessing the topographic relationship between the mandibular canal and impacted third molars. Oral Surg Oral Med Oral Pathol Oral Radiol Endod. 2007;103:253–9.
24. Kobayashi K, Shimoda S, Nakagawa Y, Yamamoto A. Accuracy in measurement of distance using limited cone-beam computerized tomography. Int J Oral Maxillofac Implants. 2004;19:228–31.
25. Lou L, Lagravere MO, Compton S, Major PW, Flores-Mir C. Accuracy of measurements and reliability of landmark identification with computed tomography techniques in the maxillofacial area: a systematic review. Oral Surg Oral Med Oral Pathol Oral Radiol Endod. 2007;104:402–11.
26. Scarfe WC, Farman AG, Sukovic P. Clinical applications of cone-beam computed tomography in dental practice. J Can Dent Assoc. 2006;72:75–80.
27. Bertram F, Bertram S, Rudisch A, Emshoff R. Assessment of Location of the Mandibular Canal: Correlation Between Panoramic and Cone Beam Computed Tomography Measurements. Int J Prosthodont. 2018;31:129–34.
28. Peltola JS, Mattila M. Cross-sectional tomograms obtained with four panoramic radiographic units in the assessment of implant site measurements. Dentomaxillofac Radiol. 2004;33:295–300.
29. Potter BJ, Shrout MK, Russell CM, Sharawy M. Implant site assessment using panoramic cross-sectional tomographic imaging. Oral Surg Oral Med Oral Pathol Oral Radiol Endod. 1997;114:436–42.
30. Vazquez L, Saulacic L, Belser U, Bernard JP. Efficacy of panoramic radiographs in the preoperative planning of posterior mandibular implants: a prospective clinical study of 1,527 consecutively treated patients. Clin Oral Implants Res. 2008;19:81–5.
31. Sghaireen MG, Srivastava KC, Shrivastava D, et al. A CBCT based three-dimensional assessment of mandibular posterior region for evaluating the possibility of bypassing the inferior alveolar nerve while placing dental implants. Diagnostics (Basel). 2020;10:E406.
32. Juodzbalys G, Wang HL, Sabalys G. Anatomy of mandibular vital structures. Part I: mandibular canal and inferior alveolar neurovascular bundle in relation with dental implantology. J Oral Maxillofac Res. 2010;1:e2.
33. Yim JH, Ryu DM, Lee BS, Kwon YD. Analysis of digitalized panorama and cone beam computed tomographic image distortion for the diagnosis of dental implant surgery. J Craniofac Surg. 2011;22:669–73.
34. Halperin-Sternfeld M, Machtei EE, Horwitz J. Diagnostic accuracy of cone beam computed tomography for dimensional linear measurements in the mandible. Int J Oral Maxillofac Implants. 2014;29:593–9.
35. Nikneshan S, Aval SH, Bakhshalian N, Shahab S, et al. Accuracy of linear measurement using cone-beam computed tomography at different reconstruction angles. Imaging Sci Dent. 2014;44:257–62.
36. Fokas G, Vaughn VM, Scarfe WC, Bornstein MM. Accuracy of linear measurements on CBCT images related to presurgical implant treatment planning: A systematic review. Clin Oral Implants Res. 2018;29:393–415.
37. Pauwels R, Stamatakis H, Bosmans H, et al. Quantification of metal artifacts on cone beam computed tomography images. Clin Oral Implants Res. 2013; 24:94–9.
38. Schulze RK, Berndt D, d'Hoedt B. On cone-beam computed tomography artifacts induced by titanium implants. Clin Oral Implants Res. 2010;21:100–7.

Publisher's Note

Springer Nature remains neutral with regard to jurisdictional claims in published maps and institutional affiliations.

Bertram *et al. BMC Med Imaging (2021) 21:46*
https://doi.org/10.1186/s12880-021-00567-7

BMC Medical Imaging

RESEARCH ARTICLE

Open Access

Implant-to-root dimensions projected by panoramic radiographs inthe maxillary canine-premolar region: implications for dental implant treatment

Annika Bertram[1], Alexander W. Eckert[2] and Rüdiger Emshoff[3,4*]

Abstract

Backgound: This study aimed to compare panoramic radiography (PAN) and cone beam computed tomography (CBCT) determinations of implant-to-root dimensions (IRD) in anterior and posterior maxillary regions, and to help determine in which instances increased radiation exposure from CBCT scans may be justified.

Methods: IRD measured by PAN (PAN-D) from implant-to-root sites (central incisor, lateral incisor, canine, first premolar, and second premolar) was collected from 418 implant sites in 110 adults. The CBCT technique was used as the reference method for the estimation of IRD. The PAN analysis equations were developed using stepwise multiple regression analysis and the Bland–Altman approach was applied to assess the agreement between PAN and CBCT methods.

Results: The odds ratio that an implant at the canine-to-first premolar (9.7:1) (P = 0.000) or at the first premolar-to-second premolar region (4.5:1) (P = 0.000) belongs to the underestimation group was strong and highly significant. The root mean square error (RMSE) and pure error (PE) were highest for the canine-to-first premolar (RMSE = 0.886 mm, PE = 0.45 mm) and the first premolar-to-second premolar region (4.5:1) (RMSE = 0.944 mm, PE = 0.38 mm).

Conclusions: This study provides evidence of site-specific underestimations of available horizontal bone dimensions for implants when assessed by PAN. These data suggest that the canines and first and second premolars may have to be excluded when assessing root angulations via PAN.

Keywords: Dental implants, Maxillary edentulousness, Panoramic radiography, Cone-beam computed tomography

Background

The success rates of implant surgery are reported to be as high as 95.1–97% [1–3]. However, surgical technique errors may occur with dental implant treatments such as abnormal implant angulations and implant malpositions [4, 5]. Furthermore, in specific regions where the implant is inserted, anatomical structures may be injured, including adjacent teeth roots, lingual and/or buccal bone plates, maxillary sinus membranes, the nasal cavity floor, and the mandibular canal [5, 6].

During implant placement, the alignment of the implant in an appropriate axial inclination to the neighboring teeth is critical for establishing and maintaining a correct and stable occlusal result. Especially in the narrow anatomical regions of the frontal maxilla, imaging

*Correspondence: ruediger.emshoff@tirol-kliniken.at
[3] University Clinic of Oral and Maxillofacial Surgery, Medical University of Innsbruck, Anichstraße 35, 6020 Innsbruck, Austria
Full list of author information is available at the end of the article

techniques that display the exact localization and morphologic relation between the critical structures are required [7].

Conventional radiographs such as panoramic radiographs provide information regarding the vertical and mesio-distal relationships of implants with neighboring teeth and adjacent anatomical structures [7]. However, panoramic radiography (PAN) is affected by a certain degree of distortion in the horizontal and vertical planes. Several in vitro [8–10] and in vivo [11, 12] investigations have assessed angular distortion in PAN images, mainly addressing the aspect of tooth inclination. These studies have shown that PAN images are of limited use to evaluate mesiodistal angulations, and variations in root angulation are described to be greatest in the maxillary canine-premolar region [8–12]. In all of these published papers [8–12], it is not clear whether the PAN magnification factor given by the manufacturers were taken into consideration to calculate the respective measurement values. Furthermore, jaw site-specific magnification factors were not considered in any of these studies, i.e., the studies failed to take into account variations in jaw size and shape and errors in positioning the jaws in the machine [13, 14].

It may be questionable to base clinical decisions regarding implant insertion in the maxillary canine-premolar region on PAN findings, as the degree of distortion described for this region may result in an incorrect diagnosis and inappropriate treatment approach being applied to the patient. Compared to PAN techniques, cone-beam computed tomography (CBCT) imaging avoids the superimpositions of neighboring structures and the disadvantage of image magnification. In addition, CBCT presents a shorter scanning time and a radiation dose up to 15 times lower than that of multislice CT [15–18]. However, according to previous studies, there is little consensus regarding how much information CBCTs can provide over conventional radiographs and in which cases increased radiation exposure can be justified [19, 20].

The purpose of the present study was to compare panoramic and CBCT determinations of implant-to–root dimensions (IRD) in anterior and posterior maxillary regions and provide clinicians with practical guidelines to help determine in which instances adjunctive use of CBCT technology may be justified.

Methods

Study design

The subjects consisted of 110 consecutive adult patients (72 females and 38 males; average age 53.0 ± 15.2 years) referred to our practice of oral and maxillofacial surgery in Freilassing, Germany, for implant surgery. The subjects were informed about the study procedure, and verbal informed consent was received from each participant. Written informed consent was waived by the Institutional Ethics Committee as data were de-identified and analysed anonymously. This retrospective study followed the medical protocols and ethics outlined in the Declaration of Helsinki and was approved by the Medical Ethical Committee of the Martin-Luther University Institutional Review Board (ethics approval No. 2020-034). The inclusion criteria were age 18 years or older, partially or totally edentulous in the maxillary anterior or premolar region, and presence of post-implant complications or additional need for dental implants warranting concurrent panoramic and CBCT images taken after the postsurgical phase of implant surgery. The exclusion criteria for the study group included the presence of metallic artifacts that could impair an accurate analysis, distorted or unclear images (e.g., artifacts, scattering), pathology in the region of interest, and complete maxillary edentulism. The patients received 418 titanium Straumann® implants (Straumann AG, Basel, Switzerland) positioned in the central incisor, lateral incisor, canine, first premolar, and second premolar region of the maxilla. All patients underwent PAN and CBCT. The CBCT technique was used as the criterion method for the estimation of IRD.

Imaging

Digital PAN was taken using the Orthophos SL 3D (ORT, Sirona Dental Systems GmbH, Germany), operating at 60–90 kVp and 3–16 mA. The magnification factor of the panoramic machine was 1.25. For CBCT imaging, the same Orthophos SL 3D machine was used. Images are rendered in a precise 1:1 ratio in the reconstruction software provided by the vendor. The scanning settings were as follows: 5 × 5.5 cm field of view, 85 kV tube voltage, 6–7 mA tube current, a radiation time of 14.1, and a 0.12 mm pixel size. By using the same protocol for all examinations performed, PAN and CBCT resulted in a radiation dose of 71 mGy cm^2 and 218 mGy cm^2, respectively. The effective dose from PAN and CBCT was 8.5 ySv and 26.2 ySv, respectively [21], i.e., the effective dose from a CBCT examination was about 3 times higher than that from the PAN examination. The radiographs were viewed with Galileos Implants and Sidexis 4.0 software (Dentsply Sirona).

Measurement procedure

Implant-to-root sites (central incisor, lateral incisor, canine, first premolar, and second premolar sites) were assessed on each panoramic and CBCT radiograph. All radiographs were analyzed in standard conditions on a high-resolution grayscale SMM Series monitor (Siemens AG, Karlsruhe, Germany).

The shortest distance from the implant to the root of the neighbouring tooth was measured with PAN at sites corresponding to the central incisor, lateral incisor, canine, first premolar, and second premolar sites. The site-specifc multiplication factor was calculated for each implant site by dividing the implant's measured length (in mm) on the postoperative PAN by the implant's real length. The CBCT distances were measured on the correspondent axialbucco-palatal slices (Figs. 1 and 2). The measurements were made by a single examiner (AB) using a digital ruler.

For assessment of site-specific intraobserver reliability, IRD in the panoramic and CBCT images of 20 randomly selected cases were evaluated and measured by the investigator on two different days. For the panoramic and CBCT measurements, the mean differences were 0.27 ± 0.24 mm and 0.19 ± 0.16 mm, respectively, and the intraclass correlation coefficient for intraobserver agreement was 0.946 and 0.966, respectively (Table 1).

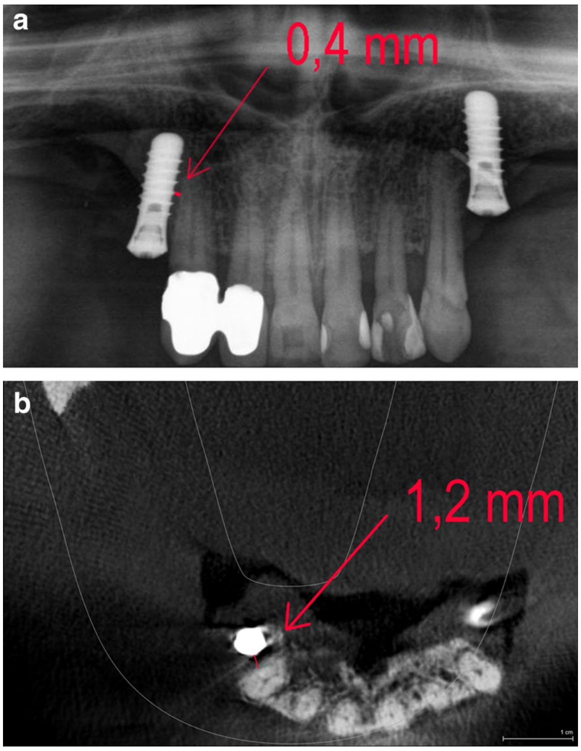

Fig. 1 IRD measuring technique on PAN (**a**) and CBCT (**b**) without overlapping structures in PAN. **a** Outer surfaces of implant and neighboring root are assessed on PAN images. At the area of smallest distance between implant and adjacent root surface the local implant thread was used as reference point for IRD measurement (red line). **b** Outer surfaces of neighboring implant and root were assessed at the level of the reference thread on axial CBCT images. IRD represents distance between implant and adjacent root surface at the level of the reference thread (red line)

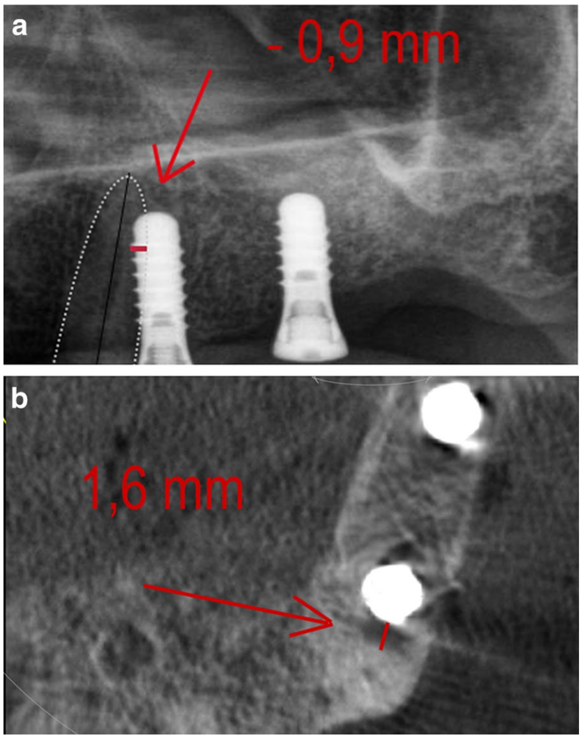

Fig. 2 IRD measuring technique on PAN (**a**) and CBCT (**b**) with overlapping structures in PAN. **a** Outer surfaces of implant and neighboring root (dotted white line) are assessed on PAN images. At the area of smallest distance, i.e. greatest overlapping distance, between implant and adjacent root surface the local implant thread was used as reference point for IRD measurement (red line). **b** Outer surfaces of neighboring implant and root were assessed at the level of the reference thread on axial CBCT images. IRD represents distance between implant and adjacent root surface at the level of the reference thread (red line)

Statistics

Apart from frequency, mean and standard deviation calculations, the statistical methods used were paired t-test and binary logistic and linear regression analyses. Binary logistic regression analysis was used for the assessment of the relative odds of each implant-to-root site. The outcome was always underestimation vs. nonunderestimation.

IRD derived from the CBCT method was used as the dependent variable for the development of prediction equations separately. The independent variables included IRD by PAN (Pan-D), age (to the nearest 1 year) and gender (male = 1, female = 0). The most predictive variables were selected by measure of goodness-of-fit statistics. A high R^2 value, and small root mean square error (RMSE) indicated the optimal model. IRD assessed by

Table 1 Site-specific intraclass correlation coefficients of duplicate PAN and CBCT measurements of implant-to-root dimensions (n = 80)

Maxillary region	n	PAN			CBCT		
		M (mm)	SD (mm)	ICC	M (mm)	SD (mm)	ICC
Cen Inc–Lat Inc	20	0.11	0.12	0.989#	0.12	0.10	0.974#
Lat Inc–Canine	20	0.78	0.66	0.966#	0.14	0.09	0.931#
Canine–1. Prem	20	0.23	0.14	0.949#	0.17	0.15	0.952#
1. Prem–2. Prem	20	0.33	0.22	0.957#	0.27	0.22	0.960#
Total	80	0.27	0.24	0.946#	0.19	0.16	0.966#

Cen central, *Lat* lateral, *Inc* incisor, *Prem* premolar, *CBCT* cone-beam computed tomography, *PAN* panoramic radiography, *n* number of sites measured, *M* mean difference between the first and second measurements, *SD* standard deviation, *ICC* intraclass correlation coefficient, *mm* millimeters

Accepted reliability

the criterion method as well as the new prediction equations were compared using one-way analysis of variance (ANOVA). The pure error (PE), calculated as the mean of squares of differences between measured and predicted values, was used to assess the performance of the prediction equations. The smaller the PE is, the greater the accuracy of the equation [11].

Moreover, the approach of Bland and Altman was used to assess the agreement between the predicted and actual IRD. This statistical approach is recognized as the most appropriate way to compare the ability of different methods to measure the same parameter [12]. The 95% limits of agreement (expressed as minus and plus 1.96 standard deviations above and below the bias) were analyzed.

Significance was set at $P < 0.05$. For the statistical analysis, the NCSS 2019 statistical software (NCSS, LLC. Kaysville, Utah, USA) was used.

Results

The distribution of the dental implants based on anatomic location is presented in Table 2. Eighty-five (20.3%) implants were inserted in the cental-lateral incisor region, 96 (23.0%) in the lateral incisor-canine region,

Table 2 Mean difference in implant-to-root dimensions by maxillary region as measured by PAN and CBCT (n = 418)

Maxillary region	n	PAN		CBCT		Difference		
		M (mm)	SD (mm)	M (mm)	SD (mm)	M (mm)	SD (mm)	P
Cen Inc–Lat Inc								
Cent Inc^I–Lat Inc^T	36	1.87	0.98	1.62	0.78	0.26	1.10	0.167
Lat Inc^I–Cent Inc^T	49	0.95	0.92	1.09	0.63	− 0.14	0.58	0.095
Total	85	1.34	1.04	1.31	0.74	0.25	0.85	0.759
Lat Inc–Canine								
Lat Inc^I–Canine^T	57	2.18	1.51	2.20	0.89	− 0.02	1.46	0.915
Canine ^{I}–Lat Inc^T	39	1.81	1.00	1.71	0.70	0.10	0.65	0.330
Total	96	2.03	1.33	2.00	0.85	0.03	1.19	0.810
Canine–1. Prem								
Canine ^{I}–1. Prem^T	41	0.30	1.12	1.54	1.00	− 1.24	1.47	0.000*
1. Prem ^{I}–Canine^T	120	0.87	1.10	1.93	1.01	− 1.06	0.91	0.000*
Total	161	0.73	1.13	1.83	1.02	− 1.11	1.08	0.000*
1. Prem–2. Prem								
1. Prem^I–2. Prem^T	41	1.10	1.40	1.63	1.31	− 0.54	0.98	0.000*
2. Prem^T–1. Prem^I	35	0.74	0.99	2.06	1.10	− 1.32	0.95	0.000*
Total	76	0.93	1.23	1.81	1.04	− 0.63	1.24	0.000*
Total	418	1.19	1.28	1.74	0.99	− 0.56	1.16	0.000*

Cen central, *Lat* lateral, *Inc* incisor, *Prem* premolar, ^{I} implant, ^{T} tooth, *CBCT* cone-beam computed tomography, *PAN* panoramic radiography, *n* number of sites measured, *M* mean, *SD* standard deviation, *mm* millimeters, *P* probability of type I error

*Significant difference with paired t-test

161 (39%) in the canine-first premolar region, and 76 (18%) in the first–second premolar region.

The mean implant-to-root dimension was 0.93 ± 1.23 mm on PAN and 1.74 ± 0.99 mm on CBCT. The difference in implant-to-root dimensions between the two radiographic techniques for the total material was − 0.56 mm ± 1.16 mm and ranged from − 1.32 mm (second premolar root-to-first premolar implant region) to 0.26 mm (central incisor-to-lateral incisor region). Statistically significant differences between the panoramic and CBCT techniques were found for the canine-to-first premolar (p = 0.000) and first premolar-to-second premolar region (p = 0.000) (Table 2).

The odds ratio that an implant at the canine-to-first premolar (9.7:1) (P = 0.000) and at the first premolar-to-second premolar region (4.5:1) (P = 0.000) belongs to the underestimation group was strong and highly significant. There was no significant increase in the odds ratio to indicate that an implant at the lateral incisor-to-canine region (0.8:1) (P = 0.493) would belong to the underestimation group (Table 3).

A single regression equation was developed for the whole sample. Gender and age were not significant predictors of IRD (P > 0.05), with PAN-D (P = 0.000) entering the model and explaining the largest variance of the models. Figure 2 shows the relationship between CBCT-D and PAN-D (R^2 = 25.6%; P = 0.000). Implant site-specific sets of preliminary equations were constructed for the prediction of CBCT-D. In each set, the equations were constructed using PAN-D as an independent variable. Implant site-specific PAN analysis prediction equations for CBCT-D were able to predict 25.0–43.4% of variances, while RMSE showed the highest values for the canine-to-first premolar (0.89 mm) and first premolar-to-second premolar region (0.94 mm) (Table 4).

The developed regression equations were applied to the sample to evaluate their accuracy. The mean absolute difference between the predicted and measured CBCT values was 0.96 ± 0.86 mm. No significant difference between measured and predicted values for each tooth region was found (P > 0.05) (range of bias, − 0.20 mm to 0.14 mm). The highest PE was found for the canine-to-first premolar (0.45 mm) and first premolar-to-second premolar region (0.38 mm). The measured values strongly correlated with the the predicted values (range of r, 0.503 to 0.674, P < 0.0001) for IRD (Table 5).

The linear relationship between the measured and predicted IRD and the difference between the measured and predicted IRD plotted against the mean of the predicted and measured IRD are shown in Figs. 3, 4, 5, 6 and 7. Bland–Altman analyses showed the lowest agreement between predicted and actual IRD for the canine-to-first premolar (limits of agreement, − 1.58 mm to 1.87 mm) and first premolar-to-second premolar region (limits of agreement, − 2.05 mm to 1.66 mm). A total of 19 implant-sites (4.6%) with

Table 3 Difference in implant-to-root dimensions by region as measured by PAN and CBCT (n = 418)

Diagnostic variables	Statistics				
	Estimate	Standard error	Odds ratio	95% CI	P
Underestimation[#]					
Lat Inc–Canine Region (n = 96)	− 2.09	0.305	0.81	0.45–1.48	0.493
Canine–1. Prem Region (n = 161)	2.30	0.339	9.95	5.12–19.31	0.000*
1. Prem–2. Prem Region (n = 76)	1.52	0.36	4.55	2.24–9.260.387	0.000*

Cen central, *Lat* lateral, *Inc* incisor, *Prem* premolar, *CBCT* cone-beam computed tomography, *PAN* panoramic radiography, *n* number of sites measured

#(PAN measurement − CBCT measurement) < 0, *P* probability of type I error

*Significant with logistic regression analysis adjusted for age and gender

Table 4 Equations for prediction of implant-to-root dimensions by region as measured by PAN and CBCT (n = 418)

Maxillary region	Equation	R^2	RMSE (mm)
Cen Inc–Lat Inc (n = 85)	CBCT-D = 1.111 + −.008 Age + .440 PAN-D	.387	.586
Lat Inc–Canine (n = 96)	CBCT-D = .663 + .010 Age + .357 PAN-D	.434	.649
Canine–1. Prem (n = 161)	CBCT-D = 1.505 + .452 PAN-D	.250	.886
1. Prem–2. Prem (n = 76)	CBCT-D = 1.232 + .641 PAN-D	.415	.944

Cen central, *Lat* lateral, *Inc* incisor, *Prem* premolar, *CBCT-D* implant-to-root dimension by cone-beam computed tomography, *PAN-D* implant-to-root dimensions by panoramic radiography, *n* number of sites measured, R^2 R square, *RMSE* root means-squared error

Table 5 Implant-to-root dimensions assessed by criterion method and each of the PAN equations (n = 418)

Maxillary region	Mean (mm)	95% CI for the mean (mm)	ANOVA[a] (P)	Correlation[b] (r)	Mean bias (mm)	Pure error (mm)
Cen Inc–Lat Inc (n = 85)						
Criterion method (CBCT)	1.3 ± 0.7	1.16–1.47				
PAN equation	1.4 ± 0.4	1.27–1.46	0.564	0.568	− 0.05 ± 0.60	0.16
Lat Inc–Canine (n = 96)						
Criterion method (CBCT)	1.9 ± 0.8	1.73–2.07				
PAN equation	1.9 ± 0.6	1.82–2.06	0.744	0.612	− 0.03 ± 0.66	0.16
Canine–1. Prem (n = 161)						
Criterion method (CBCT)	1.8 ± 1.0	1.67–1.99				
PAN equation	1.7 ± .05	1.61–1.77	0.109	0.503	0.14 ± 0.88	0.45
1. Prem–2. Prem (n = 76)						
Criterion method (CBCT)	1.8 ± 1.2	1.55–2.11				
PAN equation	2.0 ± 0.6	1.90–2.15	0.207	0.674	− 0.20 ± 0.95	0.38

CBCT cone-beam computed tomography, *PAN* panoramic radiography, *Cen* central, *Lat* lateral, *Inc* incisor, *Prem* premolar, *ANOVA* analysis of variance, *P* probability of type I error

[a] Comparison of means between criterion method and assessments made by each of the prediction equations, *r* regression coefficient

[b] Correlation between criterion method and assessments made by each of the prediction equations

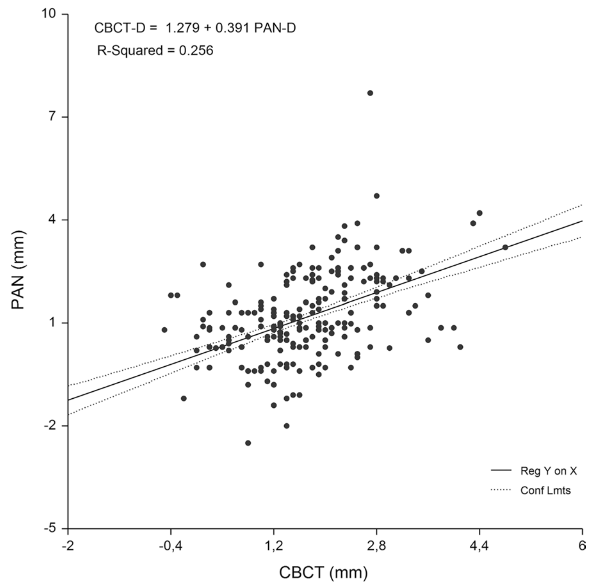

Fig. 3 Linear regression of the relationship between IRD assessed by PAN and criterion method (CBCT)

residuals exceeding the 95% confidence limits of IRD, were identified.

Discussion

The mean difference in IRDs between the two radiographic techniques was − 0.56 ± 1.16 mm. The differences between the two radiographic techniques ranged widely for IRDs. The highest negative values were found for canine-to-first premolar (− 1.11 ± 1.08 mm) and first-to-second premolar regions (− 0.63 ± 1.24 mm), i.e., PAN underestimates available horizontal bone dimensions in these regions. These findings seem to be similar to those of Tepedino et al. [22], who reported that calibrated PAN overall underestimates the available interradicular space in comparison to CBCT. However, they may contradict the reports of Bouwens et al. [11] and Peck et al. [12], who described that in comparison to CBCT, uncalibrated PAN projects the largest diversion of root angulation in the maxillary canine [11] and maxillary canine-premolar regions [12]. The findings in the latter studies [11, 12] could be contradictory because these authors did not consider the impact of jaw site-specific magnification factors, i.e., these studies failed to take into account the aspect of jaw size and shape variations and the occurrence of jaw positioning errors.

It is of clinical importance to understand and anticipate PAN-associated deviations in axial tooth positions. Significant inaccuracies in mesiodistal tooth angulations found in PAN were described by previous investigators. PAN inaccuracies have been reported to include variable vertical and horizontal magnification factors, projection geometry, focal trough depth and geometry, and positioning errors of the patient [23–26].

Several authors showed significant differences with regard to the localization of apices in the mesio-distal directions following 2D examination [27, 28]. They described a greater tendency in the first premolar region, caused by horizontal distortions on PAN images that occur in instances where the object image is located in

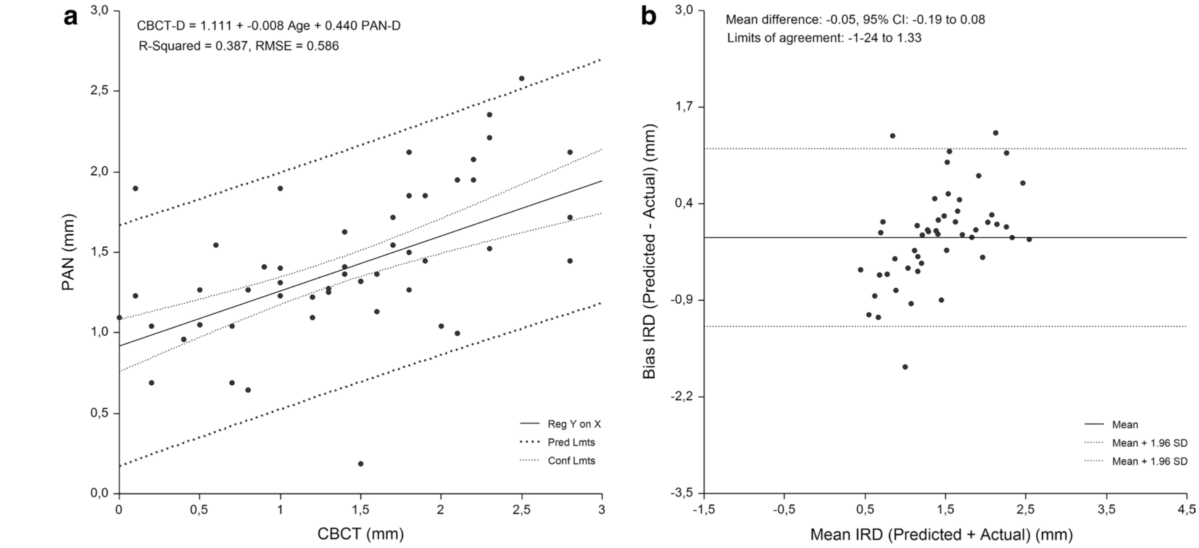

Fig. 4 Central incisor-to-lateral incisor region. Linear regression (**a**) and Bland Altman analysis (**b**) of the relationship beween IRD assessed by PAN analysis prediction equation and criterion (CBCT) method. RMSE = 0.586 mm, mean bias = -0.05 mm and PE = 0.16 mm

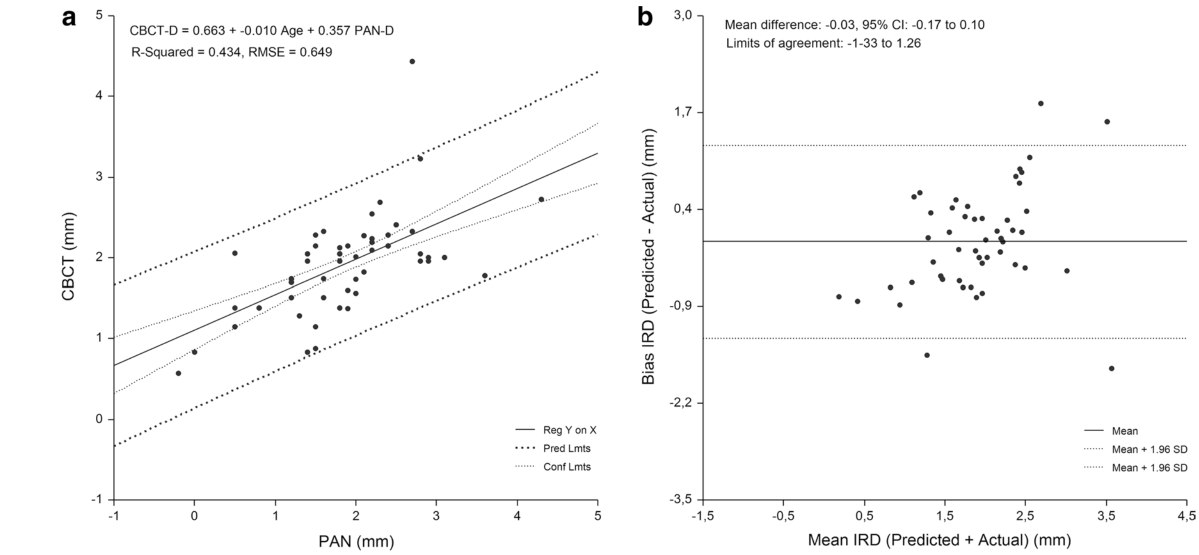

Fig. 5 Lateral incisor-to-canine region. Linear regression (**a**) and Bland Altman analysis (**b**) of the relationship beween IRD assessed by PAN analysis prediction equation and criterion (CBCT) method. RMSE = 0.649 mm, mean bias = -0.03 mm and and PE = 0.16 mm

front or behind of the focal trough [7, 29]. Furthermore, different face shapes may lead to varying maxillary dentition positionings within the focal trough, thereby causing aberrant radiographic angulations. Further investigations may be warranted to address this important issue [8].

Clinicians frequently use PAN before and during dental implant treatment to assess mesiodistal tooth angulations. The appearance of a change in mesiodistal tooth angulation may be due to varying inclinations of inserted implants and neighboring teeth in the buccolingual direction. It has been shown that an increased lingual root torque may appear as a more mesial root tip on the PAN, while an increased buccal root torque may result in a more distal root tip. Inconsistency and extensive variability have been reported regarding the effect of buccolingual angulation on mesiodistal angulation [30, 31].

PAN underestimated the available interradicular spaces in the canine-to-first premolar and first-to-second

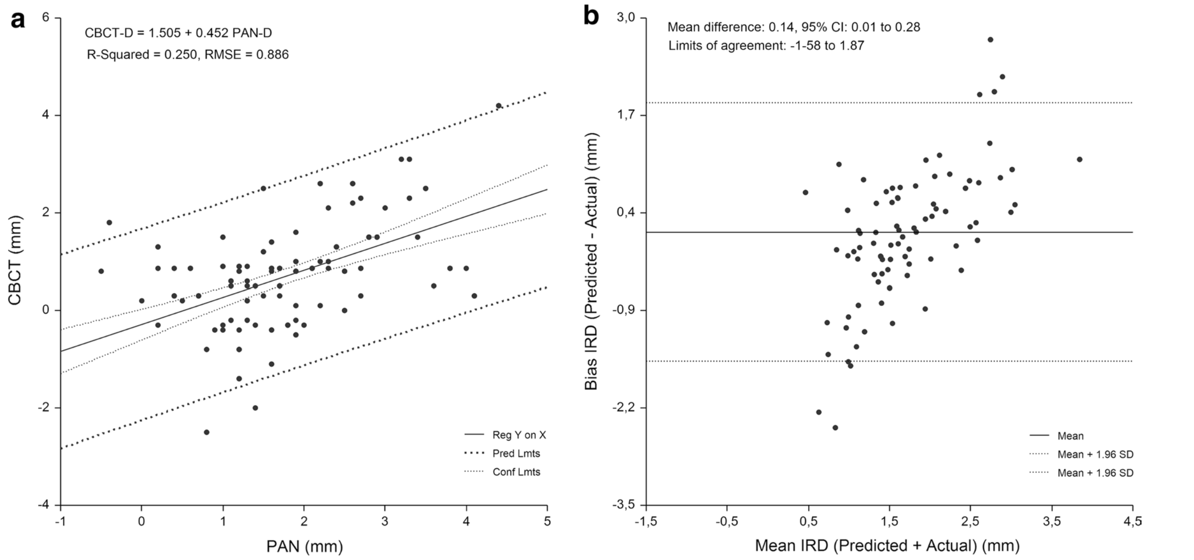

Fig. 6 Canine-to-first premolar region. Linear regression (**a**) and Bland Altman analysis (**b**) of the relationship beween IRD assessed by PAN analysis prediction equation and criterion (CBCT) method. RMSE = 0.886 mm, mean bias = 0.14 mm and PE = 0.45 mm

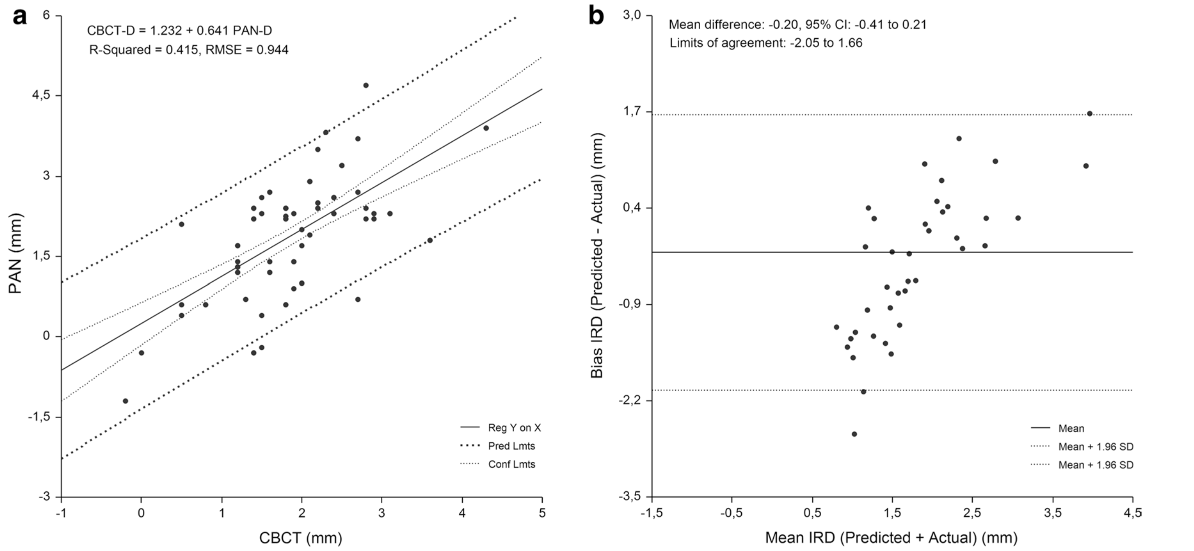

Fig. 7 First premolar-to-second premolar region. Linear regression (**a**) and Bland Altman analysis (**b**) of the relationship beween IRD assessed by PAN analysis prediction equation and criterion (CBCT) method. RMSE = 0.944 mm, mean bias = -0.20 mm, and PE = 0.38 mm

premolar regions compared with CBCT, which is considered the gold standard for linear measurements [32]. These results could be explained by the fact that the arch displays an increased curvature at the canine region, and PAN images therefore present greater distortion [10]. Furthermore, the first premolar usually has two roots and is located in a more anterior zone where the alveolar ridge is usually thinner, whereas the second premolar usually has just one root and is located in a more posterior zone where the alveolar ridge tends to widen.

It is important to insert dental implants in a functionally and esthetically correct position, i.e., dental implants must be placed in correct positions and angulations in relation to each other and to adjacent teeth. The present study provides a perspective on the contribution of tooth region variables of panoramic IRD dimensions to the occurrence of underestimation of available horizontal bone dimensions. While the lateral incisor-to-canine region contributed no amounts to the change in risk (1:0.81), a clear definition of the underestiamtion group was evident for the canine-to-first premolar (1: 9.95) and first-to-second premolar regions (1: 4.55). Therefore, based on this study, tooth region may be considered a dominant factor in the underestimation of available bone dimensions. Further investigations are indicated to clarify which additional variables may be associated with an elevated risk of underestimation of available horizontal bone dimensions.

The current study developed PAN analysis prediction equations for the estimation of IRD in the anterior and posterior maxilla. To the best of our knowledge, this is the first study to develop a PAN equation for adults across tooth region-specific groups. The developed PAN equations showed comparatively minor predictive performance for the canine-to-first premolar ($R^2 = 0.25\%$, RMSE = 0.89 mm) and the first-to-second premolar region ($R^2 = 0.42\%$; RMSE = 0.94 mm). Furthermore, the validation results indicated that PE and bias were comparatively higher for these regions, while the limits of agreement assessed by the Bland–Altman approach showed comparatively wider ranges. These data support recent changes by the American Board of Orthodontics to exclude scoring of the canines when assessing root angulations via PAN [33]. However, the data may also indicate that it would be judicious to exclude first and second premolars evaluation by PAN. Furthermore, these findings may suggest that the equations may not be suitable for use in a community or clinical setting when CBCT techniques are not available. This suggests that caution should be applied when interpreting canine, premolar, and molar angulation. Use of CBCT may therefore be recommended for all implant size and angulation estimations in these regions.

In implant dentistry, CBCT imaging has been considered a highly accurate treatment planning tool for the performance of reliable linear measurements [15, 34]. However, there are several factors, such as machine characteristics, radiation exposure, and image-processing software, that may affect the accuracy of reformatted CBCT images [35, 36]. In a recent systematic review of the available evidence on the accuracy of linear measurements when using maxillofacial CBCT specifically in the field of implant dentistry [37], the authors reported that most studies showed submillimeter accuracy of CBCT measurements compared to a gold standard, and there was no clear trend as to whether measurements are consistently under- or overestimated.

The present study needs to be evaluated in the context of some limitations. First, measurements were made by a single observer, i.e., observer bias could have occurred in the data collection process. This error may be reduced by study designs incorporating two or more observers and a multicenter setting with comparison and statistical correlation of their measurements. Second, the use of CBCT imaging can produce artifacts caused by high-density metal materials such as dental implants [38, 39], while CBCT has limited capability to decrease artifacts with use of metal artifact reduction algorithms or correct exposure settings [40, 41]. Although these artifacts occur more frequently in the mandible than in the maxilla, and are generated most prominently by zirconium implants, followed by titanium zirconium and titanium implants [42, 43], beam hardening and scattering effect artifacts could have reduced the contrast, thereby impairing the detection of structures of interest and as a result producing errors in the linear measurements on CBCT images.

Conclusions

This study provides evidence of site-specific underestimations of available horizontal bone dimensions for implants when assessed by PAN. These data may suggest that the canines andfirst and second premolars should be excluded from assessments of root angulations via PAN. Use of CBCT may therefore be recommended for all implant size and may have to be excluded from assessments of angulation estimations in these regions.

Abbreviations

ANOVA: One-way analysis of variance; CBCT: Cone-beam computed tomography; CBCT-D: IRD assessed by CBCT; IRD: Implant-to-root dimensions; PAN: Panoramic radiography; PAN-D: IRD assessed by PAN; RMSE: Root mean square error; PE: Pure error.

Acknowledgements

Not applicable.

Authors' contributions

AB and AWE conceived and designed the study. AB collected and intepreted the data. AB and RE contributed to statistical analysis and manuscript drafting. All authors read and approved the final manuscript.

Funding

Not applicable.

Availability of data and materials

Due to the nature of this research, participants of this study did not agree for their data to be shared publicly, so supporting data is not available.

Ethical approval and consent to participate

The study was approved by the Medical Ethical Committee of the Martin-Luther University Institutional Review Board (ethics approval No. 2020-034). Verbal informed consent was received from each participant.

Consent for publication

Not applicable.

Competing interests

The authors declare that they have no conflict of interest related to this article.

Author details
[1] Otto Von Guericke University of Magdeburg, Magdeburg, Germany. [2] University Clinic of Oral and Maxillofacial Surgery, Martin-Luther University, Halle-Wittenberg, Germany. [3] University Clinic of Oral and Maxillofacial Surgery, Medical University of Innsbruck, Anichstraße 35, 6020 Innsbruck, Austria. [4] Private Practice, Oral and Maxillofacial Surgery, Freilassing, Germany.

Received: 26 August 2020 Accepted: 12 February 2021
Published online: 10 March 2021

References

1. Quirynen M, de Soete M, van Steenberghe D. Infectious risks for oral implants: a review of the literature. Clin Oral Implants Res. 2020;13:1–19. https://doi.org/10.1034/j.1600-0501.2002.130101.x.
2. Goodacre CJ, Bernal G, Rungcharassaeng K, Kan JY. Clinical complications with implants and implant prostheses. J Prosthet Dent. 2003;90:121–32. https://doi.org/10.1016/S0022-3913(03)00212-9.
3. Salinas TJ, Eckert SE. In patients requiring single-tooth replacement, what are the outcomes of implant—as compared to tooth-supported restorations? Int J Oral Maxillofac Implants. 2007;22(suppl):s71–95.
4. SánchezGarcés MA, Escoda-Francolí J, Gay-Escoda C. Implant complications. Implant Dent. 2011;9:1–37. https://doi.org/10.5772/19706.
5. Misch K, Wang H-L. Implant surgery complications: etiology and treatment. Implant Dent. 2008;17:159–68. https://doi.org/10.1097/ID.0b013e3181752f61.
6. Clark D, Barbu H, Lorean A, Mijiritsky E, Levin L. Incidental findings of implant complications on postimplantation CBCTs: a cross-sectional study. Clin Implant Dent Relat Res. 2017;19:776–82. https://doi.org/10.1111/cid.12511.
7. Gratt BM. Panoramic radiography. In: Goaz PW, White SC, editors. Oral radiology: principles and interpretation. 3rd ed. St Louis: Mosby; 1994. p. 242–4.
8. Owens AM, Johal A. Near-end of treatment panoramic radiograph in the assessment of mesiodistal root angulation. Angle Orthod. 2008;78:475–81. https://doi.org/10.2319/040107-161.1.
9. Samawi SS, Burke PH. Angular distortion in the orthopantomogram. Br J Orthod. 1984;11:100–7. https://doi.org/10.1179/bjo.11.2.100.
10. Mckee IW, Williamson PC, Lam EW, Heo G, Glover KE, Major PW. The accuracy of 4 panoramic units in the projection of mesiodistal tooth angulations. Am J Orthod Dentofacial Orthop. 2002;121:166–75. https://doi.org/10.1067/mod.2002.119435.
11. Bouwens DG, Cevidanes L, Ludlow JB, Phillips C. Comparison of mesiodistal root angulation with posttreatment panoramic radiographs and cone-beam computed tomography. Am J Orthod Dentofacial Orthop. 2011;139:126–32. https://doi.org/10.1016/j.ajodo.2010.05.016.
12. Peck JL, Sameshima GT, Miller A, Worth P, Hatcher DC. Mesiodistal root angulation using panoramic and cone beam CT. Angle Orthod. 2007;77:206–13. https://doi.org/10.2319/0003-3219(2007)077[0206:MRAUPA]2.0.CO;2.
13. Mehra A, Pai KM. Evaluation of dimensional accuracy of panoramic cross-sectional tomography, its ability to identify the inferior alveolar canal, and its impact on estimation of appropriate implant dimensions in the mandibular posterior region. Clin Implant Dent Relat Res. 2012;14:100–11. https://doi.org/10.1111/j.1708-8208.2009.00226.x.
14. Gomez-Roman G, Lukas D, Beniashvili R, Schulte W. Area dependent enlargement rations of panoramic tomography on orthograde patient positioning and its significance for implant dentistry. Int J Oral Maxillofac Implants. 1999;14:248–57.
15. Scarfe WC, Farman AG, Sukovic P. Clinical applications of cone-beam computed tomography in dental practice. J Can Dent Assoc. 2006;72:75–80.
16. Kobayashi K, Shimoda S, Nakagawa Y, Yamamoto A. Accuracy in measurement of distance using limited cone-beam computerized tomography. Int J Oral Maxillofac Implants. 2004;19:228–31.
17. Loubele M, Jacobs R, Maes F, Denis K, White S, Coudyzer W, et al. Image quality vs radioation dose of four cone beam computed tomography scanners. Dentomaxillofac Radiol. 2008;37:309–19. https://doi.org/10.1259/dmfr/16770531.
18. Ziegler CM, Woertche R, Brief J, Hassfeld S. Clinical indications for digital volume tomography in oral and maxillofacial surgery. Dentomaxillofac Radiol. 2002;31:126–30. https://doi.org/10.1038/sj/dmfr/4600680.
19. Bornstein MM, Scarfe WC, Vaughn VM, Jacobs R. Cone Beam computed tomography in implant dentistry: a systematic review focusing on guidelines, indications, and radiation dose risks. Int J Oral Maxillofac Implants. 2014;29 Suppl:55–77. https://doi.org/10.11607/jomi.2014suppl.g1.4.
20. De Vos W, Casselman J, Swennen GR. Cone-beam computerized tomography (CBCT) imaging of the oral and maxillofacial region: a systematic review of the literature. Int J Oral Maxillofac Surg. 2009;38:609–25. https://doi.org/10.1016/j.ijom.2009.02.028.
21. ICRP. The 2007 recommendations of the International Commission on Radiological Protection. ICRP Publication 103. Ann ICRP. 2007;37:1–332. https://doi.org/10.1016/j.icrp.2007.10.003.
22. Tepedino M, Cornelis MA, Chimenti C, Cattaneo PM. Correlation between tooth size-arch length discrepancy and interradicular distances measured on CBCT and panoramic radiograph: an evaluation for miniscrew insertion. Dental Press J Orthod. 2018;23:39.e1-39.e13. https://doi.org/10.1590/2177-6709.23.5.39.e1-13.onl.
23. Mckee IW, Glover KE, Williamson PC, Lam EW, Heo G, Major PW. The effect of vertical and horizontal head positioning in panoramic radiography on mesiodistal tooth angulations. Angle Orthod. 2001;71:442–51. https://doi.org/10.1043/0003-3219(2001)071%3c0442:TEOVAH%3e2.0.CO;2.
24. Stramotas S, Geenty JP, Petocz P, Darendeliler MA. Accuracy of linear and angular measurements on panoramic radiographs taken at various positions in vitro. Eur J Orthod. 2002;24:43–52. https://doi.org/10.1093/ejo/24.1.43.
25. McDavid WD, Tronje G, Welander U, Morris CR. Dimensional reproduction in rotational panoramic radiography. Oral Surg Oral Med Oral Pathol. 1986;62:96–101. https://doi.org/10.1016/0030-4220(86)90079-4.
26. Scarfe WC, Nummikoski P, McDavid WD, Welander U, Tronje G. Radiographic interproximal angulations: implications for rotational panoramic radiography. Oral Surg Oral Med Oral Pathol. 1993;76:664–72. https://doi.org/10.1016/0030-4220(93)90079-j.
27. Chaushu S, Chaushu G, Becker A. Reliability of a method for the localization of displaced maxillary canines using a single panoramic radiograph. Clin Orthod Res. 1999;2:194–9. https://doi.org/10.1111/ocr.1999.2.4.194.
28. Botticelli S, Verna C, Cattaneo PM, Heidmann J, Melsen B. Two- versus three-dimensional imaging in subjects with unerupted maxillary canines. Eur J Orthod. 2011;33:344–9. https://doi.org/10.1093/ejo/cjq102.
29. Yeo DK, Freer TJ, Brockhurst PJ. Distortions in panoramic radiographs. Aust Orthod J. 2002;18:92–8.
30. Lucchesi MV, Wood RE, Nortje CJ. Suitability of the panoramic radiograph for assessment of mesiodistal angulation of teeth in the buccal segments of the mandible. Am J Orthod Dentofacial Orthop. 1988;94:303–10. https://doi.org/10.1016/0889-5406(88)90055-8.
31. Samawi SS, Burke PH. Angular distortion in the orthopantomogram. Br J Orthod. 1984;11:100–7. https://doi.org/10.1179/bjo.11.2.100.
32. Tsutsumi K, Chikui T, Okamura K, Yoshiura K. Accuracy of linear measurement and the measurement limits of thin objects with Cone Beam Computed Tomography: effects of measurement directions and of phantom locations in the fields of view. Int J Oral Maxillofac Implants. 2011;26:91–100.
33. American Board of Orthodontics. Grading system for dental casts and panoramic radiographs. American Board of Orthodontics. St. Louis: Mosby; 2012. p. 17–8.
34. Yim JH, Ryu DM, Lee BS, Kwon YD. Analysis of digitalized panorama and cone beam computed tomographic image distortion for the diagnosis of dental implant surgery. J Craniofac Surg. 2011;22:669–73. https://doi.org/10.1097/SCS.0b013e31820745a7.
35. Halperin-Sternfeld M, Machtei EE, Horwitz J. Diagnostic accuracy of cone beam computed tomography for dimensional linear measurements in the mandible. Int J Oral Maxillofac Implants. 2014;29:593–9. https://doi.org/10.11607/jomi.3409.
36. Nikneshan S, Aval SH, Bakhshalian N, Shahab S, Mohammadpour M, Sarikhani S. Accuracy of linear measurement using cone-beam computed tomography at different reconstruction angles. Imaging Sci Dent. 2014;44:257–62. https://doi.org/10.5624/isd.2014.44.4.257.

37. Fokas G, Vaughn VM, Scarfe WC, Bornstein MM. Accuracy of linear measurements on CBCT images related to presurgical implant treatment planning: a systematic review. Clin Oral Implants Res. 2018;29(suppl 16):393–415. https://doi.org/10.1111/clr.13142.
38. Pauwels R, Stamatakis H, Bosmans H, Bogaerts R, Jacobs R, Horner K, et al. Quantification of metal artifacts on cone beam computed tomography images. Clin Oral Implants Res. 2013;24:94–9. https://doi.org/10.1111/j.1600-0501.2011.02382.x.
39. Schulze RK, Berndt D, d'Hoedt B. On cone-beam computed tomography artifacts induced by titanium implants. Clin Oral Implants Res. 2010;21:100–7. https://doi.org/10.1111/j.1600-0501.2009.01817.x.
40. de-Azevedo-Vaz SL, Peyneau PD, Ramirez-Sotelo LR, Vasconcelos KF, Campos PS, Haiter-Neto F. Efficacy of a cone beam computed tomography metal artifact reduction algorithm for the detection of peri-implant fenestrations and dehiscences. Oral Surg Oral Med Oral Pathol Oral Radiol. 2016;121:550–6. https://doi.org/10.1016/j.oooo.2016.01.013.
41. Candemil AP, Salmon B, Freitas DQ, Ambrosano GM, Haiter-Neto F, Oliveira ML. Are metal artefact reduction algorithms effective to correct cone beam CT artefacts arising from the exomass? DentomaxillofacRadiol. 2019;48:20180290. https://doi.org/10.1259/dmfr.20180290.
42. Machado AH, Fardim KAC, de Souza CF, Sotto-Maior BS, Assis NMSP, Devito KL. Effect of anatomical region on the formation of metal artefacts produced by dental implants in cone beam computed tomographic images. DentomaxillofacRadiol. 2018;47:20170281. https://doi.org/10.1259/dmfr.20170281.
43. Demirturk Kocasarac H, Ustaoglu G, Bayrak S, Katkar R, Geha H, Deahl ST 2nd, et al. Evaluation of artifacts generated by titanium, zirconium, and titaniumzirconium alloy dental implants on MRI, CT, and CBCT images: a phantom study. Oral Surg Oral Med Oral Pathol Oral Radiol. 2019;127:535–44. https://doi.org/10.1016/j.oooo.2019.01.074.

Publisher's Note

Springer Nature remains neutral with regard to jurisdictional claims in published maps and institutional affiliations.

https://link.springer.com/article/10.1007/s10266-021-00632-1

Bertram, A., Eckert, A.W. & Emshoff, R. Implant-to-nasal floor dimensions projected by panoramic radiographs in the maxillary incisor–canine region: implications for dental implant treatment. *Odontology* 110, 171–182 (2022). https://doi.org/10.1007/s10266-021-00632-1

Abstract

To make a comparison of panoramic radiography (PAN) and cone-beam computed tomography (CBCT) determinations of implant-to-nasal floor dimensions (INFD) in the anterior maxillary region, and to assist in determining in which tooth regions additional radiation exposure involved in CBCT scans is justifiable. Data related to INFD by PAN (PAN-D) at implant-to-nasal floor sites (central incisor, lateral incisor, canine) were gathered using 141 implant sites from 119 adult patients. INFD was estimated employing the CBCT technique as a reference method. PAN analysis equations were created for estimation of INFD by CBCT (CBCT-D) specific to implant sites. For assessment of the agreement between the PAN and CBCT methodologies, the Bland–Altman approach was employed. There were robust and significant odds ratios that implants in the canine region would fall into the underestimation groups of > 0 mm (4.5:1) ($p = 0.003$), > 0.5 mm (6.2:1) ($p < 0.001$), and > 1 mm (5.4:1) ($p = 0.002$). The root mean squared error (RMSE) and pure error (PE) were highest for the canine region (RMSE = 1.973 mm, PE = 2.20 mm). This research offers evidence of site-specific underestimations of available horizontal bone dimensions for implants when PAN is employed to assess the availability of vertical bone dimensions. The data suggest that it may be necessary to exclude canine regions when making assessment of INFD through PAN. Use of CBCT may, therefore, be recommended for all implant size and angulation estimations in this region.

Erklärungen

(1) Ich erkläre, dass ich mich an keiner anderen Hochschule einem Promotionsverfahren unterzogen bzw. eine Promotion begonnen habe.

(2) Ich erkläre, die Angaben wahrheitsgemäß gemacht und die wissenschaftliche Arbeit an keiner anderen wissenschaftlichen Einrichtung zur Erlangung eines akademischen Grades eingereicht zu haben.

(3) Ich erkläre an Eides statt, dass ich die Arbeit selbstständig und ohne fremde Hilfe verfasst habe. Alle Regel der guten wissenschaftlichen Praxis wurden eingehalten; es wurden keine anderen als die von mir angegebenen Quellen und Hilfsmittel benutzt und die den benutzten Werken wörtlich oder inhaltlich entnommenen Stellen als solche kenntlich gemacht.

Datum, Unterschrift